Summer 1972

A Mathematical Model for Determining the Thermal Distribution Resulting from Discharge of a Heated Effluent

Alan H. Epstein
University of Central Florida

A MATHEMATICAL MODEL FOR DETERMINING THE THERMAL DISTRIBUTION RESULTING FROM DISCHARGE OF A HEATED EFFLUENT

BY

ALAN H. EPSTEIN

A Thesis Presented in Partial Fulfillment
of the Requirements for the Degree
Master of Science in Environmental Systems Management

FLORIDA TECHNOLOGICAL UNIVERSITY

August 1972

ABSTRACT

A mathematical model is presented for the problem of determining the two-dimensional temperature distribution resulting from the discharge of a heated effluent into a shallow, quiescent receptacle. The physical model for the problem is the two-dimensional jet augmented by an imposed condition of viscous drag due to bottom friction effects.

By virtue of the assumption that the physical properties of the effluent are independent of temperature over the operational temperature range of the plume, the analysis separates the total problem into a flow problem and a temperature problem. Solution of the temperature distribution is accomplished both analytically and numerically.

Analytically, the temperature distribution is found through sequential integral solution of the equations defining the mathematical model, under the physical assumptions of a Gaussian flow distribution and the following relationship between the velocity and temperature distributions:

$$\frac{T(x,y)}{T_{max}(x)} = \left[\frac{u(x,y)}{U_{max}(x)}\right]^{\frac{1}{2}}$$

where the subscript (max) denotes conditions along the jet centerline.

Numerically, the equations defining the mathematical model are solved by a finite differencing technique implemented with the aid of an I.B.M. 360 digital computer.

Comparison of the predictions of the model with the classical two-dimensional momentum jet indicate that the model is a reasonable

approximation of the real physical problem. In addition there is seen to be a critical dependence of the flow in the plume on the depth of the receptacle.

TABLE OF CONTENTS

LIST OF ILLUSTRATIONS

LIST OF SYMBOLS

Symbol	Quantity
u	Component of flow velocity in the x or downstream direction (Ft/Sec)
v	Component of flow velocity in the y or spanwise direction (Ft/Sec)
τ	Shearing stress (lb_f/Ft^2)
τ_b	Shearing stress due to bottom drag (lb_f/Ft^2)
h	Receptacle depth (Ft)
ρ	Density (lb_m/Ft^3)
g_c	Conversion constant = $32.1739 \frac{lb_m - ft}{lb_f - sec^2}$
C_f	Coefficient of viscous friction for bottom drag
Re	Reynolds Number
K	Empirical constant used in defining the shearing stress
b	Jet half width (Ft)
U, U_{max}	Centerline velocity (Ft)
C_1	Empirical constant used in defining the jet width
T	Local plume temperature (^oF)
k	Thermal diffusivity (Ft^2/Sec)
ΔQ	Net Environmental Heat Flux $\frac{BTU}{Ft^2\ sec}$
μ	Absolute viscosity $\frac{lb_m}{Ft\ sec}$
J	Joule's mechanical equivalent of heat $\frac{BTU}{(lb_m - Ft^2)/sec^2}$

Symbol	Quantity
T_D	Discharge temperature (^oF)
T_{max}	Centerline temperature (^oF)
T_{at}	Atmospheric temperature (^oF)

CHAPTER 1

INTRODUCTION

1.1 The General Problem of Industrial Waste-Heat Loads

Thermal pollution, the degradation of surface water by man-caused temperature changes, is as equally dangerous to the viability of our nation's water resources as any of the more obvious forms of water pollution. Although temperature changes may be induced indirectly through alteration of the natural heat exchange processes, as occurs in construction, irrigation, and the like, the most obvious, and indeed the most severe temperature changes result from the direct addition, or removal, of heat.

Past, present, and forecasted water requirements for purposes of cooling and condensation in the power generation and manufacturing industries indicate that discharge of industrial cooling water is the prime source of waste-heat. For example, in 1964 this type of water usage amounted to slightly over 50 trillion (50×10^{12}) gallons, approximately one-half the total water consumption in the United States for that year (1). Associated with this was a total heat rejection of some 6.8×10^{15} BTU's. More succinctly, this means that 50 trillion gallons of waste water, heated to an average of something like $14^{\circ}F$ above the ambient receptacle temperature, were discharged into the nation's surface waters in 1964.

The best predictions available to date (2,3) indicate that by the year 2000 industrial waste-heat output will be ten times that in

1964, so that the problem of thermal pollution is one of managing awesome quantities of waste-heat in a manner that will ensure the quality of our water resources.

1.2 The Effects of Thermal Pollution

It is generally conceded that temperature is among the more important parameters to be considered in the field of water quality management (4). In fact, the temperatures of surface and ground water bodies have been more extensively recorded than any other physical, chemical, or biological measurement.

The relationships of surface water temperature to aquatic life, chemical and biochemical reactions, water treatment, the toxicity of contaminants, tastes and odors in drinking water, and the quality of domestic, industrial, and agricultural water supplies have been explored by numerous investigators. However, much of the data and information obtained have not, as yet, been applied on a practical basis. Ostensibly, this is because there is a wide divergence of opinions expressed in the literature and an astounding lack of empirical field correlations. A summary of the more generally recognized effects of thermal pollution is presented in the following three sections.

1.2.1 Physical Effects

The effect of temperature on the physical properties of water has been well established for a considerable period of time. In terms of water quality, the most critical temperature dependent properties are density, viscosity, vapor pressure and the solubility of dissolved

gases, most noticeably oxygen (1). Table 1 defines the generally accepted relationships between these properties and temperature for fresh water.

The settling velocity of particles in a non-turbulent medium is given by Stoke's Law, i.e.;

$$V = \frac{d^2 g}{18\mu} (\rho_s - \rho_W)$$

where:

V = settling velocity [cm/sec]

d = diameter of settling particle [cm]

g = acceleration of gravity = 980 [cm/sec^2]

μ = viscosity of medium (water) [poises]

ρ_s = density of settling particle [gm/cm^3]

ρ_W = density of water [gm/cm^3]

As temperature increases, the combined effect of water density and viscosity is to increase settling velocity. In turn, an increase in settling velocities has a significant effect on the amount and location of sediment and sludge deposition in sluggish rivers, reservoirs, and estuaries.

Evaporation is forced by the differences in temperature and water vapor pressure between the water body and its overlaying layer of air. Obviously, the higher the temperature of the water body, the higher its corresponding evaporation flux, for a fixed air temperature.

Thermal stratification, caused by very slight differences in water density, inhibits vertical mixing and, therefore, oxygen transfer

TABLE 1 (1)

WATER PROPERTIES

TEMPERATURE [F^0]	DENSITY [GM/CM]	ABS. VISCOSITY [Centipoises]	PRESSURE [mm Hg]	DISSOLVED OXYGEN SATURATION [MG/L]
32	.99987	1.7921	4.58	14.6
41	.99999	1.5188	6.54	12.8
50	.99973	1.3077	9.21	11.3
59	.99913	1.1404	12.8	10.2
68	.99823	1.0050	17.5	9.2
77	.99707	.8937	23.8	8.4
86	.99567	.8007	31.8	7.6
95	.99406	.7225	42.2	7.1

to the lower water levels. A difference of .001 in specific gravity is sufficient to cause a stable stratification in quiescent water bodies (5,6).

Because of the dependence of virtually all life forms on oxygen, the relation of water temperature to gas solubility is a critically important aspect of thermal pollution. The solubility of oxygen in water is directly proportional to its partial pressure at equilibrium conditions with the atmosphere. Hence, temperature increases proportionally decrease the oxygen holding capacity of a water body, thereby reducing its life support capabilities.

1.2.2 Chemical Effects

By far and away, the most significant aspect of temperature variations in a viable surface water body involve the resulting changes in reaction rates and degree of reaction completion for the bio-chemical reactions of indigenous life processes. In general, bio-chemical reactions follow the van't Hoff Rule of a doubling of reaction rate for a $10^{\circ}C$ increase in temperature (7). For any chemical reaction to be considered complete, the rate of forward reaction must be equal to the rate of reverse reaction. Both the time required to reach equilibrium and the relative proportion of reactants and products at equilibrium are strong functions of temperature.

Taste and odor problems associated with accelerated anaerobic bacterial activity are accentuated by oxygen depletions due to temperature increases. In addition, tastes and odors are generally more

noticeable in warmer water due to decreased solubility of methane and hydrogen sulfide, the products of anaerobic decomposition.

The biochemical oxygen demand (B.O.D.), or rate of oxygen uptake for purposes of bacterial respiration and other bio-chemical processes, exerted by a bio-degradable organic load is satisfied in a much shorter time at increased temperatures due to the increased intensity of microbial activity. This means that an excessive oxygen depletion might occur where at lower temperatures it would have been avoided.

1.2.3 Biological Effects

Any viable surface water body is a highly complex ecological system and, as such, virtually defies generalized statements as to the effects of temperature changes on aquatic biota. For example, temperatures which are not directly lethal to a particular species may affect reproduction or growth, or may reduce important food organisms, inducing an imbalance in the system which may eventually seriously endanger the species in question. As a result, the great majority of available literature is directed at investigation of locally important species. A brief summary of the effects of thermal pollution on the more prevalent forms of aquatic life follows.

Fish are poikilothermic animals, that is, they normally take on the temperature of their ambient environment. In a majority of fish species the body temperature differs from ambient water temperature by only about 1.0-2.0^{o}F (8,9). The consequences of this are twofold;

1. There is a critical dependence on temperature in the host-pathegen relationship in fishes and,
2. It is a fundamental requirement of fishes that the external temperature be well suited to fish tissue functionality.

Generally, temperature changes have been seen to affect metabolism, disease, reproduction, growth and development, and location and distribution of fishes (1).

The number and variety of aquatic bacterial species is very large, and their effects vary from potential lethality to organic waste stabilization. The temperature of natural waters in the United States is usually below the optimum for pollution associated bacteria. Increasing the water temperature increases bacterial growth if available food and oxygen are sufficient. If the food supply is limited and temperature is increased, the die-off rate increases. Again, oxygen depletion caused by increased temperature may cause organically loaded water to go septic.

Because the photosynthetic process in water is highly temperature sensitive, thermal pollution has a decided effect on the propagation and growth of algae and other aquatic plant life. In turn this affects taste, odor, and B.O.D., important water quality parameters.

1.3 A Specific Aspect of Thermal Pollution - The Thermal Mixing Zone

Although numerous problems of detail can be identified under the general category of thermal pollution, most can be classified as

sub-topics in one of two major areas. The first of these is the physical, chemical, and biological effects of increased temperature from a heated discharge. The second is the prediction and field verification of physical dispersion patterns, or the thermal plume.

As indicated in the previous sections of this chapter, although there is still need for additional work, the physical, chemical, and biological effects of increasing the average temperature of a viable body of water are reasonably well defined. Indeed, legislated federal and state water standards have already begun to develop a pattern of regulation through the establishment of criteria quantifying allowable thermal discharges and ultimate receptacle temperature limits (10). Hence, the most pressing need in this area appears to be implementation of these criteria into a consolidated national program of thermal water quality management along with unified enforcement procedures.

In contrast, a methodology for predicting the thermal dispersion pattern resulting from a waste-heat outfall has yet to be made available on a readily applicable basis. Inasmuch as this dispersion pattern defines the thermal mixing zone, and hence the area of maximum man-caused energy transfer to natural water bodies, the importance of its analytical quantification to thermal pollution control is manifest.

The most rigorous definition of the thermal mixing zone, and the one adopted for reference within the framework of this paper, is as follows: the thermal mixing zone is that area of mixing needed for the thermal plume to reach some accepted fraction of ambient natural water temperatures (11).

1.4 Analytical Treatment of the Thermal Plume in the Literature

In the past few years there have been several attempts to analyze the thermal plume problem. In each case, the governing equations have been taken to be resultant from the fundamental equations of fluid dynamics and heat transfer; that is, the equations of continuity and momentum conservation, and the fluidic energy equation augmented by a net heat flux summation through the air-water interface (12, 13, 14, 15). The complexity of the requisite mathematics has, to date, prohibited any sort of closed form analytical solution to the general problem, although there is a considerable body of work relating to specialized cases.

The most outstanding examples of available literature, and those which are most representative of the available spectrum of analytical approaches, are the papers by McLay et al (12), Giles et al (13), Stolzenbach and Harleman (14), and Koh (15).

Both the papers by McLay and Giles employ numerical simulations which require the use of a high speed digital computer. McLay et al simulate the thermal effects of a nuclear plant discharge by assuming three distinct plume regions: the open channel at the outfall, the mixing regime immediately adjacent to the entry and, the area of flow in which the plume assumes the flow pattern of the ambient receptacle. The summation of these three regions is taken to represent the total thermal plume.

Giles et al numerically solve the three dimensional diffusion equation, augmented by the use of meteorological data, wind, and wave induced currents as forcing functions. The accuracy of the model is

seen to be good, however, the requisite empirical data necessary for a prediction is exhaustive.

Stolzenbach and Harleman (14) present an approximate theoretical development which assumes the discharge is a three-dimensional turbulent jet with an unsheared initial core and a turbulent region in which the velocity and temperature distributions are related to center-line values by similarity functions.

Finally, Koh (15) analyzes the dispersion of heat resulting from a two-dimensional, horizontal surface discharge into a quiescent receptacle body. Included in the analysis are the effects of discharge momentum, plume bouyancy, entrainment, and interfacial shear.

It should be noted here, that while the results of each of the investigations cited were reasonably accurate for the particular physical situation analyzed, each ignored one parameter or another which has significance to the completely general case. Most noticeably, each paper neglected the viscous effects of bottom drag on the plume flow distribution, an omission which has a fair amount of significance to the fluid motion involved, as will be shown.

1.5 Scope of the Present Study

The temperature distribution resulting from the discharge of a heated effluent into a shallow, quiescent receptacle body is analyzed. The physical model for the analysis is the free two-dimensional momentum jet experiencing a viscous drag due to bottom friction effects. Mathematically, the model is implemented through the solution of the two-dimensional momentum transport equation augmented by bottom shear-

ing stress, and the two-dimensional energy equation, augmented by the net physical heat exchange rate between the plume and its ambient environment.

1.6 Objective of the Present Study

The objective of the present study is two-fold:

1. To provide a concise methodology which will permit the prediction of waste-heat outfall temperature distributions in shallow, quiescent, surface water bodies with reasonable accuracy and at a minimum expenditure of time and money.
2. To provide the analytical basis for future work in predicting the temperature distribution in the general thermal plume.

CHAPTER 2

THE THERMAL PLUME PROBLEM

2.1 Introduction

Problems involving the transfer of heat within a fluid flow exhibit a high degree of interaction between the thermal and flow phenomena, the heat flow superimposing itself on the physical motion of the fluid. In the general case this interaction is mutual, the temperature distribution being dependent on the velocity distribution and conversely, the velocity distribution being dependent on the temperature distribution. However, where the properties of the fluid are assumed to be independent of temperature, mutual interaction ceases and the velocity field becomes independent of the temperature field, although the converse dependence of the temperature field on the velocity field still persists (16).

Because the overriding flow mechanism in the high temperature area of an effluent thermal plume is a forced momentum transfer, the assumption that fluid properties are independent of temperature is generally well taken. Consequently, the problem of determining the thermal distribution in waste-heat outfalls becomes one of determining the flow distribution and then applying it to a mass-energy balance to determine the temperature distribution (16).

2.1.1 The Flow Problem

The physics involved in discharging an effluent into a shallow receptacle is amply described by the efflux of a two-dimensional jet

from an orifice, augmented by a locally imposed viscous drag due to bottom friction effects. In turn, the physical flow problem may be considered an example of two-dimensional fluidic motion in the absence of solid boundaries to which may be applied the boundary layer theory (16). The assumption of two-dimensionality implies a uniformity of flow throughout the depth of the receptacle over the operational area of the plume. Because the receptacle is shallow (i.e. is of the same depth as the orifice), and because the flow emerging from the orifice is almost immediately turbulent, insuring good vertical mixing in the critical high temperature region, this assumption appears reasonable.

The emerging jet carries with it some of the surrounding fluid which was originally at rest due to friction developed on the jet periphery. The resulting pattern of streamlines, as well as the coordinate system adopted for the jet, is shown in Figure 1.

The jet spreads outward in the downstream direction whereas its velocity in the center decreases in the same direction. Both effects are due to friction. The pressure gradient in the x-direction is neglected because the constant pressure of the receptacle is assumed to impress itself on the jet (16).

2.1.2 The Temperature Problem

The temperature distribution resulting from the energy balance defining the effluent outfall is a function of the fluid momentum transport, as defined by the flow problem, and the physical processes of energy exchange with the environment. These include radiation to

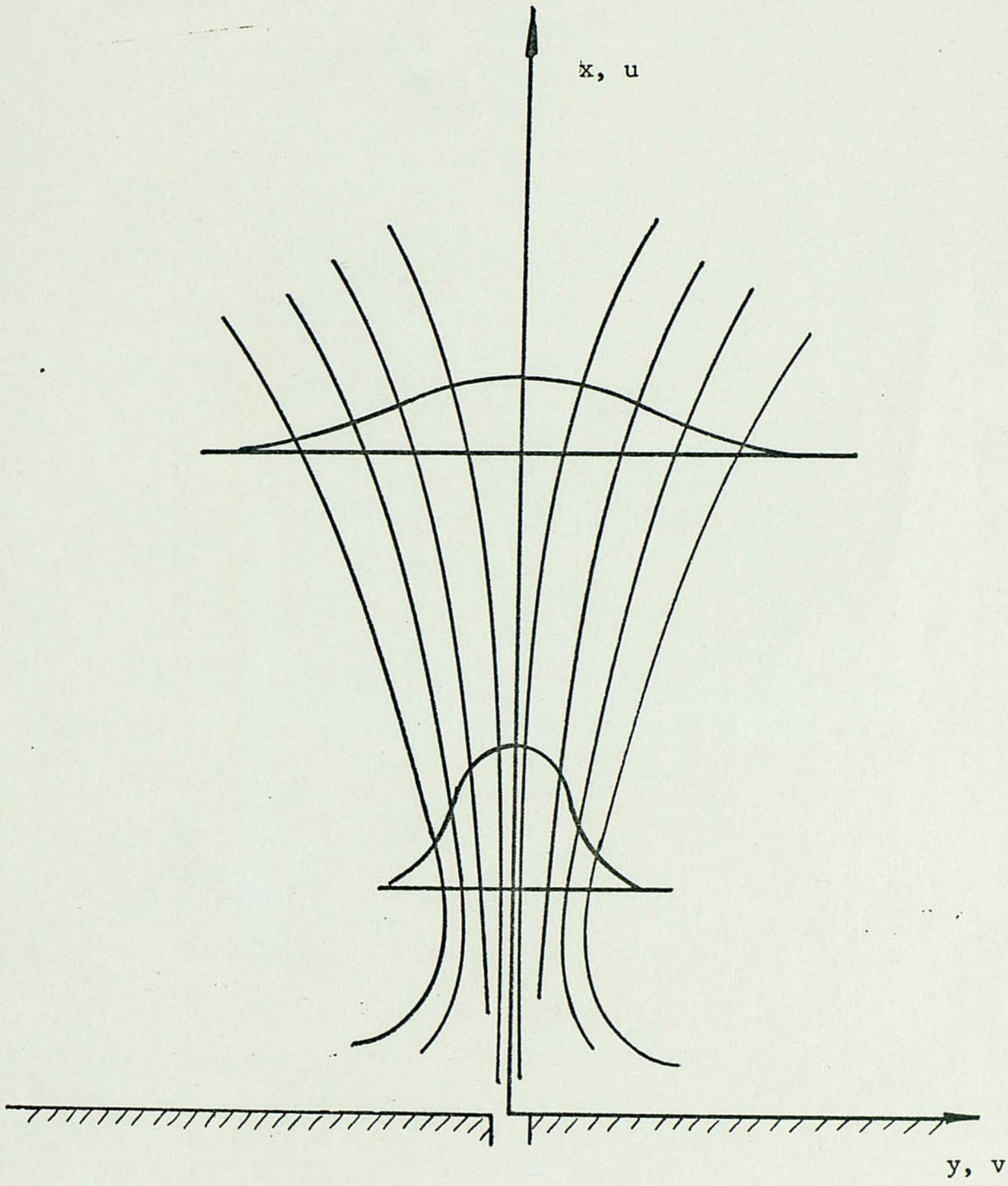

Fig. 1.--The Two Dimensional Momentum Jet

and from the plume surface, convection at the surface, conduction at the periphery, and evaporation at the air-water interface. Because the receptacle floor is saturated with water from the plume, it is assumed to be at the ambient plume temperature. Hence, heat exchange here is negligible.

The net radiative heat flux consists of total incident radiation from the sun, reduced by atmospheric attenuation, less the reflected flux, less radiation from the plume surface. In general, it is a function of solar attitude, atmospheric turbidity, cloud cover, relative atmospheric humidity, and water temperature.

The evaporative and convective heat fluxes are functions of water temperature, water vapor pressure, and wind speed. A more detailed discussion of the radiative, convective, and evaporative heat fluxes, and their defining parameters is presented in section 2.3.1 of this chapter.

2.2 Analysis of the Flow Problem

The assumptions and approximations governing the flow analysis as presented are as follows:

1. The flow is steady state, incompressible, and two-dimensional.
2. The receptacle is quiescent, that is, it has no fluid velocity.
3. The spanwise velocity distribution in the plume is Gaussian.
4. The physical properties of the fluid are independent of temperature over the operational area of the plume.
5. The pressure gradient in the flow direction is negligible.

Under the above assumptions the equations of motion defining the flow problem are as follows;

Momentum Conservation:

$$u \frac{\partial u}{\partial x} + v \frac{\partial u}{\partial y} = g_c/\rho \left[\frac{\partial \tau}{\partial y} - \frac{\tau_b}{h} \right] \qquad (2.1)$$

Continuity:

$$\frac{\partial u}{\partial x} + \frac{\partial v}{\partial y} = 0$$

where:

u = Component of flow velocity in x-direction (ft./sec.)

v = Component of flow velocity in y-direction (ft./sec.)

τ_b = Shearing stress due to viscous effects of bottom drag (lb_f/ft^2)

h = Average depth of the receptacle (ft.)

ρ = Density of effluent (lb_m/ft^3)

g_c = Dimension conversion constant = 32.1739 $\left(\frac{lb_m - ft}{lb_f - sec^2} \right)$

For the sake of complete clarity as to the physical meaning of the terms in equation 2.1, a derivation is presented in the following section.

2.2.1 Development of the Momentum Equation

The ensuing development is patterned after that of Kays (17). The essential difference here is the inclusion of the term (τ_b/h) which is taken to represent the average shearing stress over the plume depth h, caused by viscous fluid motion over the bottom of the receptacle. By allowing the bottom shear to be averaged over the plume depth the incorporation of the effects of a vertical velocity gradient is made

possible without destroying the simplifying two dimensionality of the flow model.

Consider the differential fluid element dx dy within the plume, as shown in Figure 2.

Summing forces in the x-direction yields:

$$\Sigma F_x = h[\tau\, dx + (\sigma_x + \frac{\partial \sigma_x}{\partial x} dx)dy] - h[\sigma_x\, dy + (\tau + \frac{\partial \tau}{\partial y} dy)dx - (\tau_b/h)dxdy]$$

or

$$\Sigma F_x = [\frac{\partial \sigma_x}{\partial x} - \frac{\partial \tau}{\partial y} + \tau_b/h]h\, dy\, dx \qquad (2.3)$$

In section 2.1 and 2.2 it was assumed that the constant pressure of the receptacle impresses itself on the jet. Therefore:

$$\frac{\partial \sigma_x}{\partial x} = -\frac{dP}{dx} = 0$$

so that:

$$\Sigma F_x = -[\frac{\partial \tau}{\partial y} - \frac{\tau_b}{h}]dx\, dy\, h \qquad (2.4)$$

Because momentum in the x-direction is conserved,

$$\text{Momentum}_x = g_c F_x; \quad (2.1a)$$

where:

$$\Sigma M_x = [G_y u dx + G_x u dy]h - [G_x u + \frac{\partial (G_x u)}{\partial x} dx]hdy - [G_y u + \frac{\partial (G_y u)}{\partial y} dy]\, hdx$$

or

$$\Sigma M_x = -\left[\frac{\partial (G_y u)}{\partial y} + \frac{\partial (G_x u)}{\partial x}\right] h\, dx\, dy \qquad (2.5)$$

From the equation of continuity:

$$\frac{\partial G_x}{\partial x} + \frac{\partial G_y}{\partial y} = 0$$

so that equation (2.5) becomes:

$$\Sigma M_x = -\left[\left(G_x \frac{\partial u}{\partial x}\right) + \left(G_y \frac{\partial u}{\partial y}\right)\right] h\, dx\, dy \qquad (2.6)$$

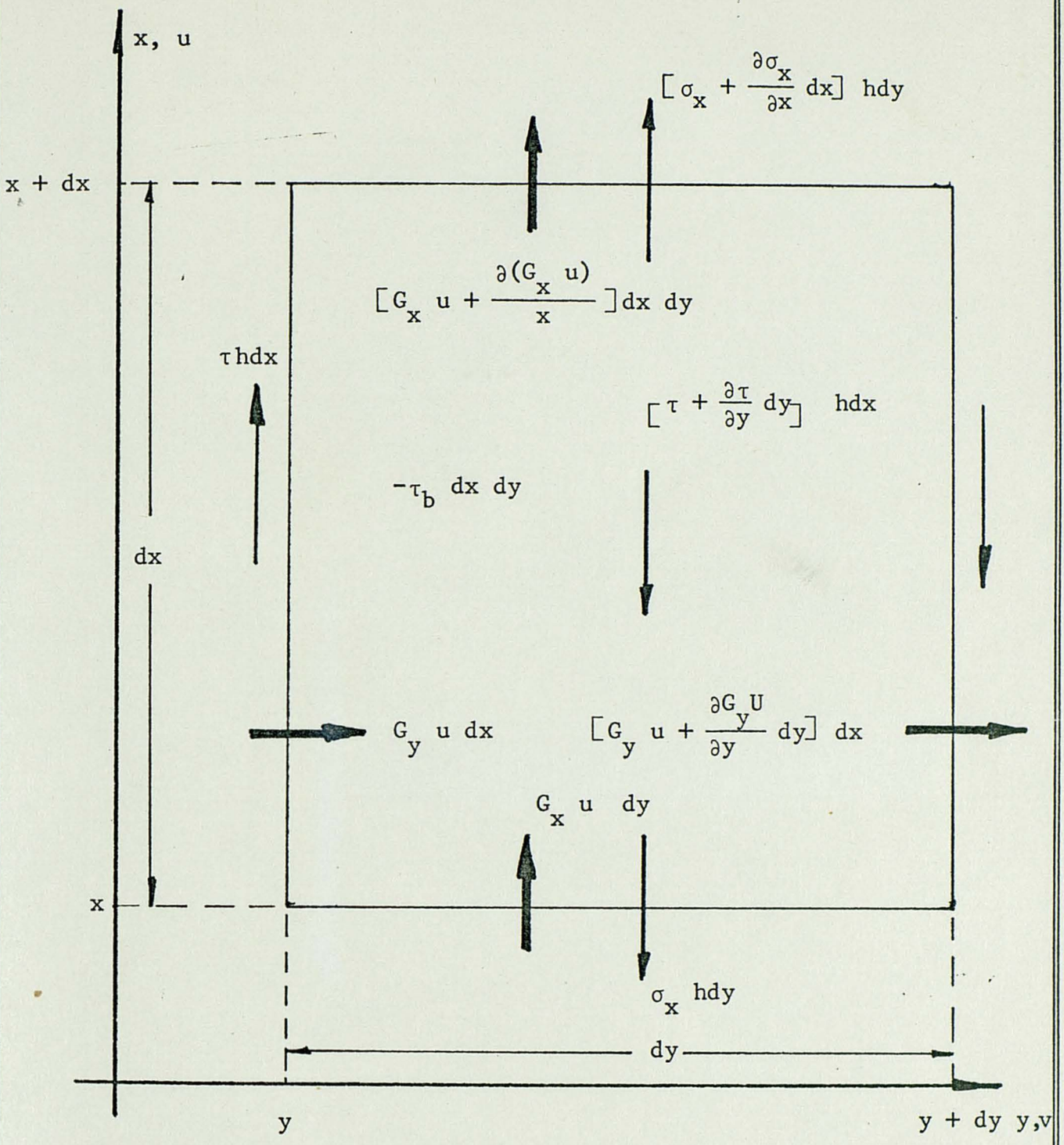

where:

G = mass flux; $\frac{lb_m}{Sec\ Ft^2}$

τ = shearing stress; $\frac{lb_f}{Ft^2}$

σ = P = normal stress as pressure; $\frac{lb_f}{Ft^2}$

Fig. 2.--The Differential Fluid Element dx dy

Substituting equations (2.4) and (2.6) into equation (2.1a) yields:

$$-\frac{1}{g_c}\left(G_x \frac{\partial u}{\partial x} + G_y \frac{\partial u}{\partial y}\right) hdxdy = -\left(\frac{\partial \tau}{\partial y} - \frac{\tau_b}{h}\right) hdxdy \qquad (2.1b)$$

Now:

$$G_x = (\rho\, u)$$

$$G_y = (\rho\, v)$$

so that equation (2.1b) becomes:

$$(1/g_c)(\rho u \frac{\partial u}{\partial x} + \rho v \frac{\partial u}{\partial y}) = \frac{\partial \tau}{\partial y} - \frac{\tau_b}{h}$$

which is identically equation (2.1).

2.2.2 An Approximate Analytical Solution to the Flow Problem

The general methodology involved in the solution of the equations of motion of the flow problem follows the von Karmen integral method and is as follows. The velocity distribution across the plume is assumed to be Gaussian, allowing for direct integration of the momentum equation over y. It is noted that the assumption of a Gaussian velocity distribution is an approximation for the problem under consideration. However, sufficient empirical correlation for the two-dimensional jet exists in the literature (16, 17) to warrant the assumption for purposes of this analysis. The integration reduces the original second order partial differential equation to a first order ordinary differential equation which is solved for the complete two-dimensional velocity distribution of the plume. For the sake of

brevity and continuity of the development, intermediate mathematical manipulations involved in the solution are presented in Appendix A.

Consider again equations (2.1) and (2.2), the equations of motion:

$$u \frac{\partial u}{\partial x} + v \frac{\partial u}{\partial y} = \left(g_c/\rho\right) \left(\frac{\partial \tau}{\partial y}\right) - \left(g_c/\rho\right)\left(\frac{\tau_b}{h}\right) \tag{2.1}$$

$$\frac{\partial u}{\partial x} + \frac{\partial v}{\partial y} = 0 \tag{2.2}$$

With the aid of equation (2.2) it can be shown that:

$$\int_0^b v \frac{\partial u}{\partial y}\, dy = \int_0^b u \frac{\partial u}{\partial x}\, dy \tag{2.7}$$

where b is the jet half-width (ft.). Integrating the left hand side of equation (2.1) and making the substitution of equation (2.7) yields:

$$\int_0^\infty \left(u \frac{\partial u}{\partial x} + v \frac{\partial u}{\partial y}\right) dy = 2\int_0^b u \frac{\partial u}{\partial x}\, dy \tag{2.8}$$

The right hand side of equation (2.1) represents the net shearing effect of the fluid motion. It is necessary that two cases be considered here; turbulent and laminar flow. For both cases the mathematical representation of the shear at the jet periphery and bottom shear follow Schlicting (16). They are as follows:

For the laminar case;

$$\tau = \frac{\mu}{g_c} \frac{\partial u}{\partial y} \tag{2.9}$$

$$\tau_b = \frac{\rho u^2 (.664)}{2 g_c (Re)^{\frac{1}{2}}}$$

For the turbulent case;

$$\tau = \frac{\rho K b (U - u) \frac{\partial u}{\partial y}}{g_c} \tag{2.11}$$

$$\tau_b = \frac{\rho u^2 (.074)}{2 g_c (Re)^{1/5}} \tag{2.12}$$

Where:

μ = viscosity; (lb_m/ft-sec)

Re= Reynolds Number = $\frac{\rho u x}{\mu}$; (dimensionless)

K = empirical constant

b = jet half-width; (ft)

U = centerline velocity of the jet; (ft/sec)

Substituting equations (2.9), (2.10), (2.11), and (2.12) into the right hand side of equation (2.1) and integrating yields:

For the turbulent case;

$$\int_0^\infty \left[\left(\frac{g_c}{\rho} \right) \left(\frac{\partial \tau}{\partial y} \right) - \left(\frac{g_c}{\rho} \right) \left(\frac{\tau_b}{h} \right) \right] dy =$$

$$Kb \left[\int_0^b \left[\frac{\partial^2 u}{\partial y^2} (U - u) - \left(\frac{\partial u}{\partial y} \right)^2 \right] dy \right] - \frac{.037}{h} \int_0^b \frac{u^2}{\left[\frac{\rho u x}{\mu} \right]^{1/5}} dy \tag{2.13}$$

For the laminar case;

$$\int_0^\infty \left[\left(\frac{g_c}{\rho} \right) \left(\frac{\partial \tau}{\partial y} \right) - \left(\frac{g_c}{\rho} \right) \left(\frac{\tau_b}{h} \right) \right] dy =$$

$$\mu(\rho) \int_0^b \frac{\partial^2 u}{\partial y^2} dy - \frac{.332}{h} \int_0^b \frac{u^2}{\left[\frac{\rho u x}{\mu} \right]^{1/2}} dy \tag{2.14}$$

A Gaussian velocity distribution is now assumed across the plume as depicted in Figure 3, i.e.

$$u/U = e^{a(y/b)^2}$$

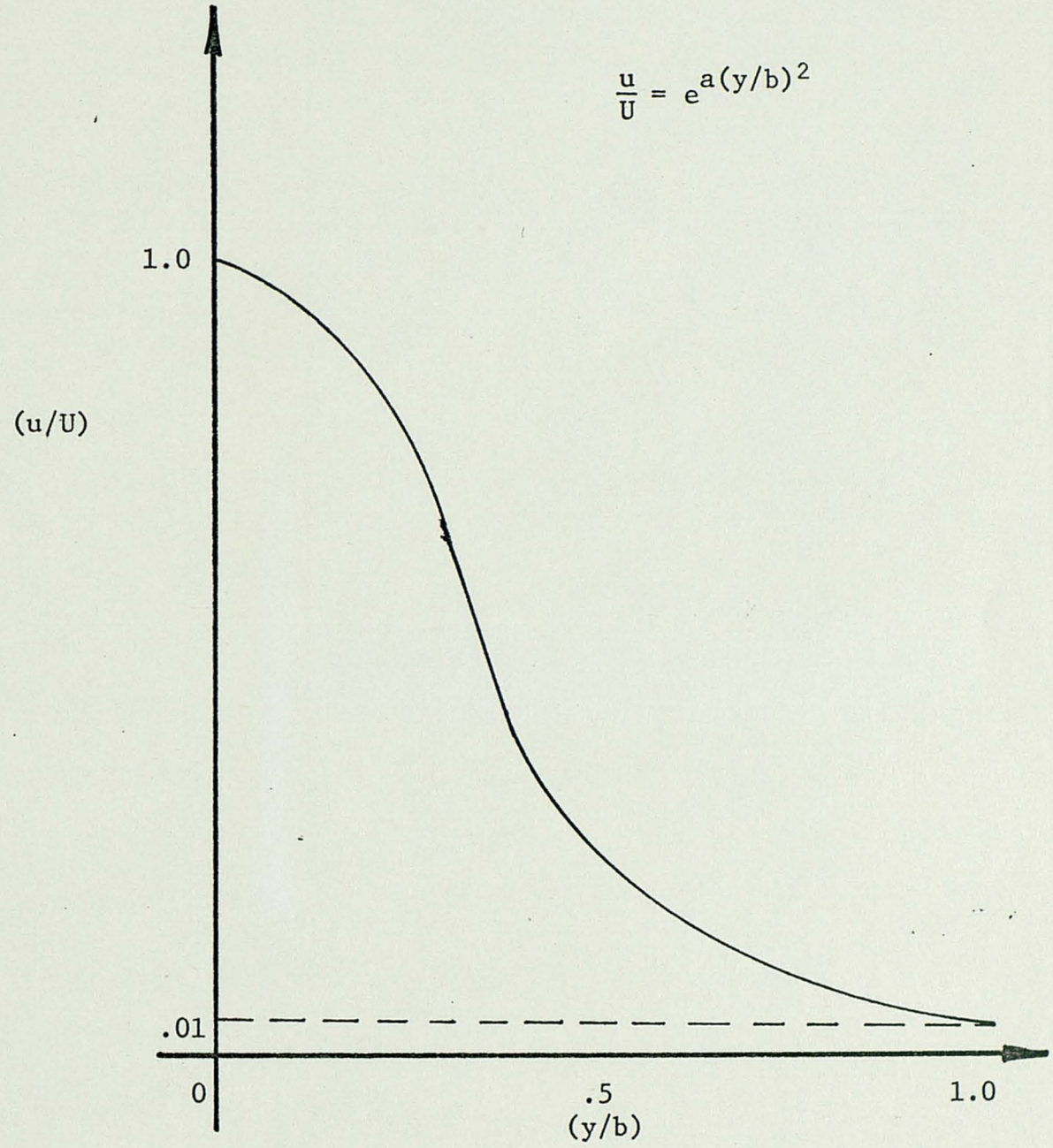

Fig. 3.--The Gaussian Velocity Distribution

The boundary conditions for the velocity distribution are:

$$@ \quad y/b = 0.0; \quad \frac{u}{U} = 1.0$$

$$\text{and } @ \quad y/b = 1.0; \quad \frac{u}{U} = .01$$

These conditions determine the value of the constant a, that is;

$$a = -4.606$$

So that the velocity distribution across the plume is:

$$\frac{u}{U} = e^{-4.606(y/b)^2} \tag{2.15}$$

The principle of conservation of mass, as applied to the problem at hand implies;

$$\rho \int_0^b u \, dy = \text{const.}$$

or, combining with the assumption of a Gaussian velocity distribution

$$2.84 \; U(0) \; b(0) = U(x) \; b(x) \tag{2.16}$$

where the (0) denotes conditions at the orifice and the (x) denotes conditions at any arbitrary point on the downstream centerline.

Substituting equation (2.15), and its appropriate derivatives, and equation (2.16) into equations (2.13), (2.14), and (2.8), combining terms, and integrating over y, the second order partial differential momentum equation is reduced to an ordinary first order differential equation i.e.;

For the turbulent case:

$$C \frac{dU}{dx} e^{AU^2/c^2} + \frac{B}{U} \frac{dU}{dx}$$

$$= DU^2 + \frac{EU^2 b}{\left[\frac{\rho U x}{\mu}\right]^{1/5}} \tag{2.17}$$

and for the laminar case;

$$C \frac{dU}{dx} e^{AU^2/c^2} + \frac{B}{U} \frac{dU}{dx}$$

$$= F \frac{U}{b} + \frac{GU^2 b}{\left[\frac{\rho U x}{\mu}\right]^{\frac{1}{2}}} \qquad (2.18)$$

where:

$$A = -9.212$$

$$B = \frac{.75C^2}{\left[9.212\right]^{\frac{1}{2}}}$$

$$C = 2.84\ U(0)\ b(0)$$

$$D = -.04K$$

$$E = -\frac{.00925}{h}$$

$$F = -.04\ \frac{\mu}{\rho}$$

$$G = -\frac{.095}{h}$$

Schlicting (16) notes that the rate at which the width of the mixing zone increases with the distance x, for the classical jet, may be expressed as follows:

$$b = c_1 x \qquad (2.19)$$

where c_1 is a constant.

Equation (2.19) is a semi-empirical relationship which has been demonstrated for the classical two-dimensional jet and, as such, is an approximation to the problem under consideration. Theoretically, it is unnecessary to make this approximation, the combination of equations (2.17) and (2.18) with equation (2.16) completely defining the centerline velocity distribution, U(x). However, the use of

equation (2.19) at this point makes equation (2.17) a separable first order ordinary differential equation which can be solved with comparative ease relative to the equation generated through the use of equation (2.16). In addition there is sufficient empirical correlation for equation (2.19) to make its use as an approximation reasonable within the scope of this analysis.

Making the substitution of equation (2.19) in equation (2.17) yields:

$$\frac{C}{U^2}\frac{dU}{dx}e^{AU^2/C^2} + \frac{B}{U^3}\frac{dU}{dx} = D + Hx \qquad (2.20)$$

where:

$$H = -\frac{.00925(.196)}{h\left[\frac{\rho C}{\mu(.196)}\right]^{1/5}}$$

Equation (2.20) is a separable, first order ordinary differential equation and is solved as follows:

$$C\int \frac{e^{AU^2/C^2}}{U^2}\,dU + B\int \frac{1}{U^3}\,dU = D\int dx + H\int x\,dx \qquad (2.21)$$

Performing the indicated integration yields

$$-\frac{B}{U^2} = Dx + \frac{H}{2}x^2 + \text{const}$$

or, solving for U:

$$U = \left[\frac{-B}{Dx + \frac{H}{2}x^2}\right]^{\frac{1}{2}} + C_2 \qquad (2.22)$$

where the constant is evaluated as follows:

$$@ \quad x = 0 \quad ; \quad U = U(0)$$

Evaluating the constant yields:

$$C_2 = 0$$

Making the substitution of equation (2.22) into equation (2.15) yields:

$$u = \left[\frac{-B}{Dx + \frac{H}{2}x^2}\right]^{\frac{1}{2}} e^{-4.606(y/.196x)^2} \qquad (2.23)$$

Equation (2.23) represents the complete two-dimensional velocity distribution for the turbulent case of the flow problem; where

$$B = \frac{.75C^2}{[9.212]^{\frac{1}{2}}}$$

$$D = -.04\ K$$

$$H = -\frac{.00925\ (.196)}{h\left[\frac{\rho C}{\mu(.196)}\right]^{1/5}}$$

$$K = .037$$

$$C = 2.84\ U(0)\ b(0)$$

By the mathematical procedure used to reduce equation (2.17) to equation (2.23), equation (2.18) may also be reduced. However, due to the additional complexities introduced by flow transition, and because its effect is experienced only by those areas in the plume where there happens to be a relatively low thermal potential, the case of laminar flow is omitted here.

Having obtained an analytical expression for the centerline velocity distribution, i.e. equation (2.22), it is possible to obtain,

with the aid of equation (2.16), an analytical expression for the jet width as a function of downstream distance from the orifice, x. That is;

$$b = C\left[\frac{Dx + Hx^2}{-B}\right]^{\frac{1}{2}}$$

In turn, it is theoretically possible to increase the accuracy of the analytical solution by using the above expression for the jet width as an approximation to a first order iteration on the solution represented by equation (2.23). This would be accomplished by replacing equation (2.19) with the above expression and generating a new solution for the centerline velocity distribution.

2.3 Analysis of the Thermal Problem

Under the assumptions and approximations outlined in sections 2.1 and 2.2, the differential equation defining the temperature problem is the two-dimensional energy equation, as presented by Schlicting (16), augmented by a net heat flux term representing the total energy exchange between the plume and its ambient environment, i.e.;

$$u\frac{\partial T}{\partial x} + v\frac{\partial T}{\partial y} = \frac{\partial}{\partial y}\left(k\frac{\partial T}{\partial y}\right) + \frac{\mu J}{\rho Cp}\left(\frac{\partial u}{\partial y}\right)^2 + \frac{\Delta Q}{h\rho Cp} \qquad (2.24)$$

where:

T = Temperature; (^{o}F)

k = Thermal diffusivity; (ft^2/sec)

J = Joule's mechanical equivalent of heat; $\left[\frac{BTU}{(lb_m\text{-}ft^2)/(sec^2)}\right]$

Cp = Specific heat at constant pressure; ($BTU/lb_m\text{-}^{o}F$)

$\frac{\Delta Q}{h_\rho C_p}$ = Net external heat flux; ($^{o}F/sec$)

2.3.1 The Energy Equation

The solution of equation (2.24) requires that the term representing the net external heat flux, Q, be defined in terms of water temperature and the empirically determined parameters which comprise the component heat fluxes. Following Zeller (18);

$$\Delta Q = \left[Qs - Qh - Qe + \frac{Qv}{2.78 \times 10^{-4}}\right] 2.78 \times 10^{-4} \qquad (2.25)$$

where:

Qs = net radiation flux, defined as

$Qs = (1 - .0071\ C^2)\ (Qi - Qr)$

where:

C = cloud cover in tenths

Qi = incident radiation

Qr = reflected radiation

The net radiation flux is independent of plume temperature, so that empirical values of Qi and Qr will provide the most accurate estimates of Qs.

It should be noted here that Qi, the incident radiation flux, is a strong function of solar attitude, and, therefore, terrestrial lattitude and season of the year. These factors must be given consideration in choosing a value for Qi.

Qh = heat convected from the plume surface, defined as

$$Qh = .00407\ VP(T_{at} - T_w)$$

where:

V = wind speed; (knots)

P = atmospheric pressure; (in. Hg)

T_{at} = air temperature; (^{o}F)

T_w = local water temperature within the plume; (^{o}F)

Qe = heat loss to evaporation, defined as

$$Qe = 12\ V(p_w - p_a);\ \left[\frac{BTU}{Ft^2 - Hr}\right]$$

where:

V = wind speed; (knots)

p_w = saturation water vapor pressure at water surface temperature;(in. Hg)

p_a = atmospheric water vapor pressure; (in. Hg)

While, in the strictest sense, p_w is a function of water temperature, for purposes of analysis it is assumed to be

independent of temperature; the value taken at the estimated average plume temperature being considered valid over the entire operational range of the plume.

Qv = advected heat input, defined as

$$Qv = \left[\rho\ U(0)\right] \quad \left[Cp\ [T_d - T_{wa}]\right]$$

where:

$\rho\ U(0)$ = effluent mass flux; $\left[\frac{lb_m}{ft^2 - sec}\right]$

Cp = specific heat

T_d = discharge temperature

T_{wa} = ambient water temperature of the receptacle outside the plume area;

Here again, Qv is independent of the local plume temperature, being a function of the boundary conditions of the physical problem.

Making the above substitutions in equation (2.25) and then applying equation (2.25) to equation (2.24), the energy equation defining the temperature problem becomes

$$u\frac{\partial T}{\partial x} + v\frac{\partial T}{\partial y} = \frac{\partial}{\partial y}\left[k\frac{\partial T}{\partial y}\right] + \frac{\mu J}{\rho Cp}\left(\frac{\partial u}{\partial y}\right)^2 + \frac{2.78 \times 10^{-4}}{h\ Cp}\{Qc - .00407\ VP\ (Ta - T)\} \tag{2.26}$$

where:

$$Qc = (Qs - Qe)a + Qv$$

$$a = 2.78 \times 10^{-4}$$

Here, as with the momentum equation, it becomes necessary to consider two cases: laminar and turbulent flow. For the case of laminar flow, the thermal diffusivity, k, is defined as

$$k = \frac{\sigma}{\rho Cp} \; ; \; \frac{Ft^2}{Sec} \tag{2.27}$$

where:

$$\sigma = \text{Thermal conductivity}; \left[\frac{BTU}{sec - Ft - {}^{o}F}\right]$$

For turbulent flow the Reynold's analogy suggests a total thermal diffusivity of the form,

$$k = \frac{\sigma}{\rho Cp} + Kb(U - u) \; ; \left[\frac{Ft^2}{Sec}\right] \tag{2.28}$$

All other terms in equation (2.26) enjoy general applicability, and remain the same for both laminar and turbulent flow.

2.3.2 An Approximate Analytical Solution to the Temperature Problem

The basis for the analytical solution to the temperature problem lies in the fact that there is an experimentally demonstrated relationship between the temperature and velocity distributions in free momentum jets. Consequently, the general methodology employed for solving the flow problem is used to solve the temperature problem.

Schlicting (16) gives the empirical relation between the temperature and velocity distribution as:

$$\frac{T}{Tmax} = \left[\frac{u}{U}\right]^{\frac{1}{2}} \tag{2.29}$$

where:

T_{max} is the temperature distribution along the jet axis (i.e. where y = 0); $T_{max} = T_{max}(x)$

T is the temperature anywhere within the plume; $T = T(x,y)$

Here once again, it must be noted that equation (2.29) has been demonstrated for the classical two-dimensional jet and is therefore an approximation for the case under consideration.

Making the substitution of equation (2.15) yields:

$$\frac{T}{T_{max}} = e^{-2.303(y/b)} \tag{2.30}$$

By defining the function $T_{max}(x)$ in equation (2.30), the complete two-dimensional temperature field, T(x,y), is defined.

Consider equation (2.26), the energy equation, i.e.:

$$u \frac{\partial T}{\partial x} + v \frac{\partial T}{\partial y} = \frac{\partial}{\partial y}\left(K\frac{\partial T}{\partial y}\right) + \frac{\mu J}{\rho Cp}\left(\frac{\partial u}{\partial y}\right)^2 + \frac{2.78 \times 10^{-4}}{h\rho Cp}\{Qc - .00407\ VP(T_{at} - T)\} \tag{2.31}$$

Along the line y = 0 (the x-axis), the following conditions apply

@ y = 0;

$$v = 0$$

$$u = U$$

$$\frac{\partial u}{\partial y} = 0$$

$$\frac{\partial T}{\partial y} = 0$$

$$T = T_{max}$$

so that equation (2.31) becomes

$$U \frac{dT_{max}}{dx} = M[Qc - N\ (T_{at} - T_{max})] \qquad (2.32)$$

substituting for the centerline velocity distribution and integrating yields:

$$(1/MN)\ln\ [MQc - MN(T_{at} - T_{max})]$$

$$= \left[-\frac{2B}{H}\right]^{\frac{1}{2}} \ln\ \left[x + \frac{D}{H} + \frac{2D}{H}\, x + x^{\frac{1}{2}}\right] + C_3 \qquad (2.33)$$

where:

$$M = \frac{2.78 \times 10^{-4}}{h\rho Cp}$$

$$N = .00407\ VP$$

$$B = \frac{.75C^2}{(9.212)^{\frac{1}{2}}}$$

$$D = -.04K$$

$$H = -\frac{.00925(.196)}{h\left[\frac{\rho C}{\mu(.196)}\right]^{1/5}}$$

$$C = 2.84\ U(0)\ b(0)$$

C_3 = Constant of integration, evaluated as follows:

$$@ \quad x = 0; \quad T_{max} = T_D$$

where T_D is the temperature of the effluent at discharge. Evaluating the constant yields:

$$C_3 = \left(\frac{1}{MN}\right) \ln \left[MQc - MN(T_{at} - T_D)\right] + \left[\frac{2B}{H}\right]^{\frac{1}{2}} \ln \frac{D}{H} \qquad (2.34)$$

It is noted here that equation (2.33 is for the case of turbulent flow. For reasons presented in section 2.2.2 of this chapter the laminar case is omitted.

Now letting;

$$\Gamma(x) = [MN]\left[-\frac{2B}{H}\right]^{\frac{1}{2}} \ln \left[x + \frac{D}{H} + \left(\frac{2D}{H}x + x^2\right)^{\frac{1}{2}}\right] + \ln \left[MQc - MN(T_{at} - T_D)\right] + MN \left[\frac{2B}{H}\right]^{\frac{1}{2}} \ln \frac{D}{H} \qquad (2.35)$$

And solving for T_{max}, equation (2.33) becomes;

$$T_{max} = e^{[\Gamma(x)]} - MQc + MNT_{at} \qquad (2.36)$$

where equation (2.36) represents the centerline temperature distribution for the turbulent case of the thermal plume. Making the substitution of equation (2.36) in equation (2.29) gives the complete two-dimensional temperature distribution for the turbulent jet, i.e.;

$$T = \left[e^{(\Gamma(x))} - MQc + NMT_{at}\right] e^{-2.303(y/b)} \qquad (2.37)$$

2.4 A Numerical Analysis of the Thermal Plume Problem

The analytical solution of the thermal plume problem, as presented in sections 2.2.2 and 2.3.2 of this chapter, requires that several empirical relationships demonstrated for the classical two-dimensional momentum jet be employed as approximations to the problem under consideration. By finite differencing the fundamental equations of momentum and energy transport, i.e. equations (2.1) and (2.2), and employing a computational grid which describes the plume as a mesh of interconnecting nodes for each of which the conditions of conservation of momentum, continuity, and conservation of energy are satisfied, it is possible to eliminate these approximations from the analysis. However, despite the elimination of the physical assumptions of the Gaussian velocity distribution and equation (2.19), the numerical analysis is not exact due to the inherent approximations envoked by the finite differencing scheme. The numerical approach is widely used in momentum-energy transport problems and has been demonstrated to give results in good agreement with empirical correlations (21,22).

2.4.1 The Finite Differenced Momentum Equation and the Computational Cell for the Flow Problem

The partial differential equation defining the flow problem, as developed in section 2.2.1 of this chapter, is as follows:

$$u \frac{\partial u}{\partial x} + v \frac{\partial u}{\partial y} = (g_c/\rho) \left(\frac{\partial \tau}{\partial y} - \frac{\tau_b}{h} \right) \quad ; \qquad (2.1)$$

where:

For the case of laminar flow:

$$\tau = \frac{\mu}{g_c} \frac{\partial u}{\partial y}$$

$$\tau_b = \frac{\rho u^2 C_f}{2g_c} \quad ; \quad C_f = .664\ Re^{-\frac{1}{2}}$$

For the case of turbulent flow:

$$\tau = \frac{\rho K b}{g_c} (U - u) \frac{\partial u}{\partial y}$$

$$\tau_b = \frac{\rho u^2 C_f}{2g_c} \quad ; \quad C_f = .074\ Re^{-1/5}$$

Consider now the finite fluid element $\Delta x\ \Delta y$, as shown in Figure 4, to which equation (2.1) is applied. Applying the central differencing technique to the appropriate terms in equation (2.1), for cell (i,j) yields:

$$u = u_c$$

$$v = v_\sigma$$

$$\frac{\partial u}{\partial x} = \frac{u_a - u_f}{2\Delta x}$$

$$\frac{\partial u}{\partial y} = \frac{u_d - u_e}{2\Delta y}$$

$$\frac{\partial^2 u}{\partial y^2} = \frac{u_d + u_e - 2u_c}{4(\Delta y)^2}$$

Substituting the above expressions into equation (2.1) and making the appropriate substitutions for the shearing stresses yields:

$$u_c \left[\frac{u_a - u_f}{2\Delta x}\right] + v_\sigma \left[\frac{u_d - u_e}{2\Delta y}\right] =$$

$$Kb \left[(U-u_c) \left[\frac{u_d + u_e - 2u_c}{4(\Delta y)^2}\right] - \frac{(u_d - u_e)^2}{4(\Delta y)^2}\right]$$

$$- \frac{u_c^2 C_f}{2h} \qquad (2.38)$$

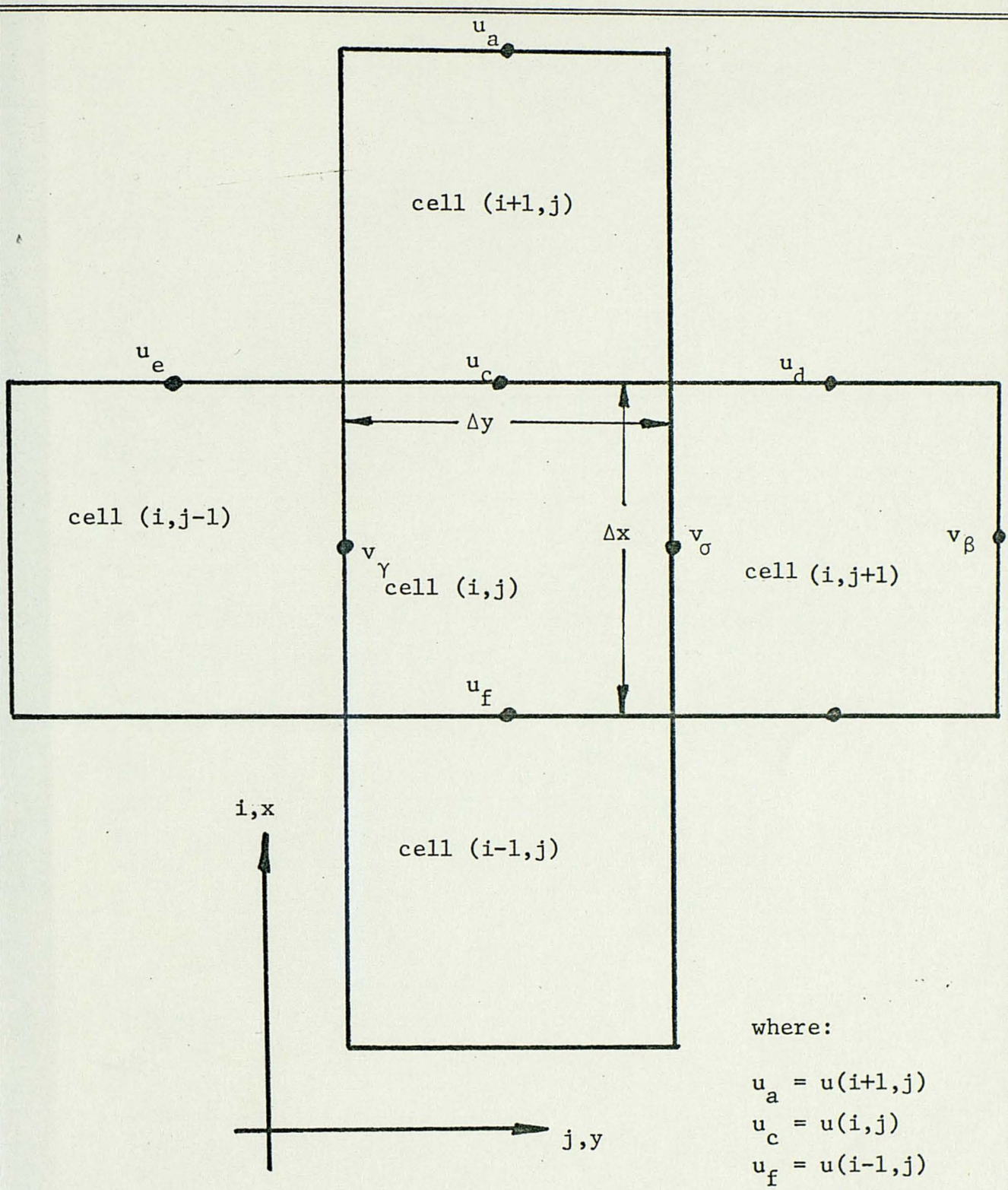

where:

$u_a = u(i+1,j)$
$u_c = u(i,j)$
$u_f = u(i-1,j)$
$u_d = u(i,j+1)$
$u_e = u(i,j-1)$
$v_\sigma = v(i,j)$
$v_\beta = v(i,j+1)$
$v_\gamma = v(i,j-1)$

Fig. 4.--The Computational Cell Structure For The Flow Problem

For the case of turbulent flow, while for laminar flow:

$$u_c \left[\frac{u_a - u_f}{2\Delta x} \right] + v_\sigma \left[\frac{u_d - u_e}{2\Delta y} \right] = \frac{\mu}{\rho} \left[\frac{u_d + u_e - 2u_c}{4(\Delta y)^2} \right]$$

$$- \frac{u_c^2 C_f}{2h} \quad ; \qquad (2.39)$$

Equations (2.38) and (2.39) completely define the finite differenced form of the momentum equation.

2.4.2 The Finite Differenced Energy Equation and the Computational Cell For the Thermal Problem

The partial differential equation defining the temperature problem is presented in section 2.3.1 of this chapter and is as follows:

$$u \frac{\partial T}{\partial x} + v \frac{\partial T}{\partial y} = \frac{\partial}{\partial y} \left(k \frac{\partial T}{\partial y} \right) + \frac{\mu J}{\rho Cp} \left(\frac{\partial u}{\partial y} \right)^2$$

$$+ \frac{2.78 \times 10^{-4}}{h \rho Cp} \{ Q_c - .00407 \, VP \, (T_{at} - T) \} \qquad (2.26)$$

where, for turublent flow:

$$k = \frac{\sigma}{\rho Cp} + Kb \, (U - u)$$

and, for the laminar flow case:

$$k = \frac{\sigma}{\rho Cp}$$

Consider again the finite fluid elements $\Delta x \, \Delta y$, as presented in Figure 5, to which equation (2.26) is applied. Again, as with the

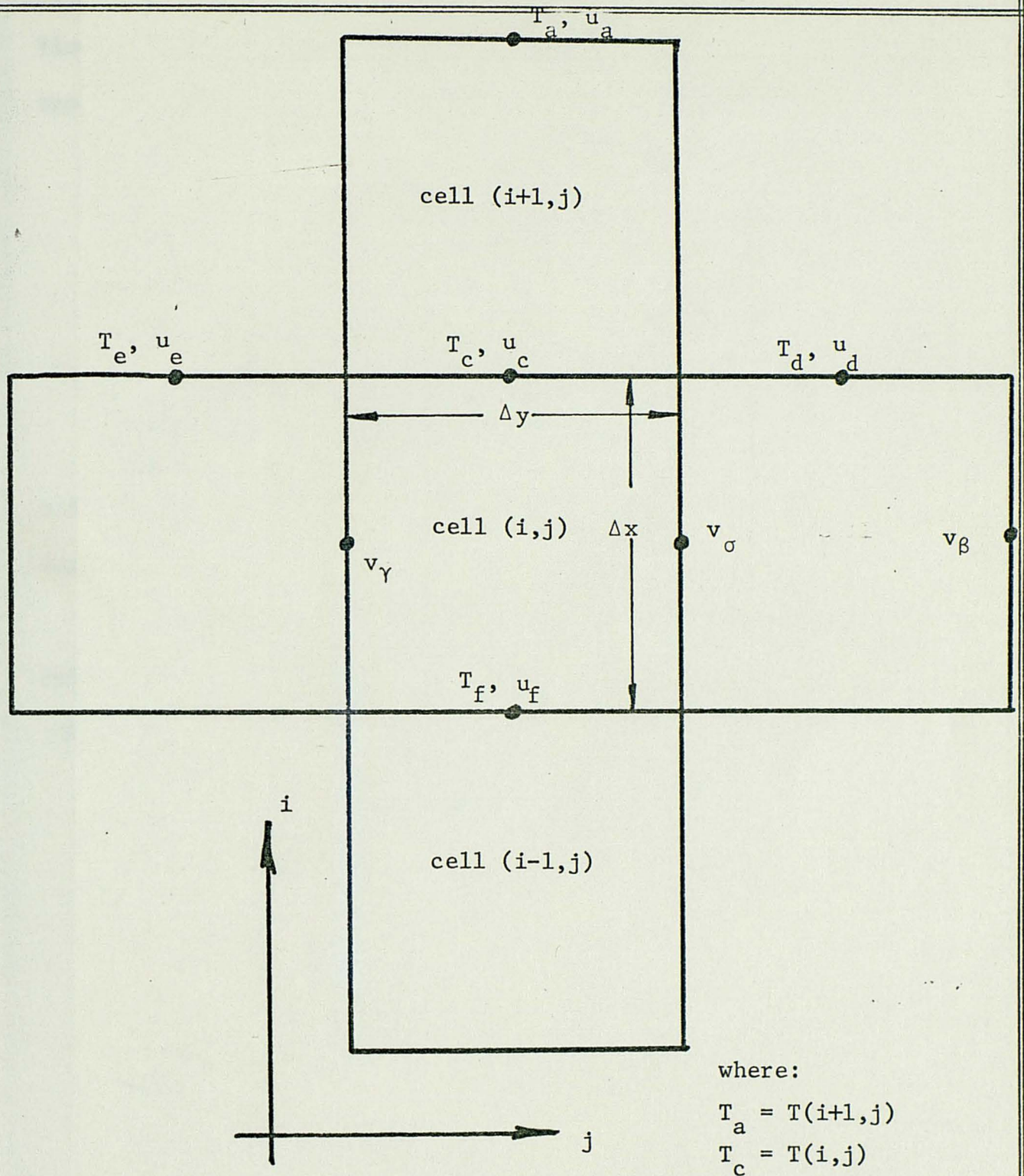

where:

$T_a = T(i+1,j)$

$T_c = T(i,j)$

$T_f = T(i-1,j)$

$T_d = T(i,j+1)$

$T_e = T(i,j-1)$

and the u and v velocity components defined as in Figure 4.

Fig. 5.--The Computational Cell Structure For The Temperature Problem

flow problem, applying the central differencing technique to the appropriate terms in equation (2.26), for cell (i,j), yields:

$$T = T_c$$

$$\frac{\partial T}{\partial x} = \frac{T_a - T_f}{2\Delta x}$$

$$\frac{\partial T}{\partial y} = \frac{T_d - T_e}{2\Delta y}$$

$$\frac{\partial^2 T}{\partial y^2} = \frac{T_d + T_e - 2T_c}{4(\Delta y)}$$

with the flow velocities and their appropriate derivatives as defined for the flow problem.

Substituting the above expressions into equation (2.26) and making the appropriate substitutions for the thermal conductivities yields:

$$u_c \left(\frac{T_a - T_f}{2\Delta x}\right) + v_\sigma \left(\frac{T_d - T_e}{2\Delta y}\right) =$$

$$\frac{\sigma}{\rho Cp}\left[\frac{T_d + T_e - 2T_c}{4(\Delta y)^2}\right]$$

$$+ Kb \left[(U - u_c)\frac{T_d + T_e - 2T_c}{4(\Delta y)^2}\right.$$

$$\left. - \frac{(T_d - T_e)(u_d - u_e)}{4(\Delta y)^2}\right]$$

(2.40)

$$+ \frac{\mu J}{\rho Cp}\frac{(u_d - u_e)^2}{4(\Delta y)^2} + \frac{2.78 \times 10^{-4}}{h\rho Cp}\{Qc - .00407\ VP(T_{at} - T_c)\};$$

For the case of turbulent flow, while for laminar flow:

$$u_c \left(\frac{T_a - T_f}{2\Delta x}\right) + v_\sigma \left(\frac{T_d - T_e}{2\Delta y}\right)$$

$$= \frac{\sigma}{\rho Cp} \frac{T_d + T_e - 2T_c}{4(\Delta y)^2}$$

$$+ \frac{\mu J}{\rho Cp} \frac{(u_d - u_e)^2}{4(\Delta y)^2}$$

$$+ \frac{2.78 \times 10^{-4}}{h\rho Cp} \{Q_c - .00407\ VP\ (T_{at} - T_c)\}\ ; \qquad (2.41)$$

Equations (2.40) and (2.41) completely define the finite differenced form of the energy equation.

2.4.3 The Computational Scheme

The general methodology involved in the solution of the finite differenced forms of the momentum and energy transport equations requires the direct sequential solution of equations (2.38), (2.39), (2.40) and (2.41) for each computational cell within the nodal mesh. Values from previously calculated cells or constraints of the physical problem serve as boundary conditions. In addition, both the velocity and thermal gradients are considered to be linear within a range of one elemental dimension on either side of a given node.

It should be noted here that equation (2.39), (i.e. the finite differenced momentum equation for the case of laminar flow) is used in place of equation (2.38) where the flow for a particular cell within the grid is determined to be laminar based upon a local Reynolds number

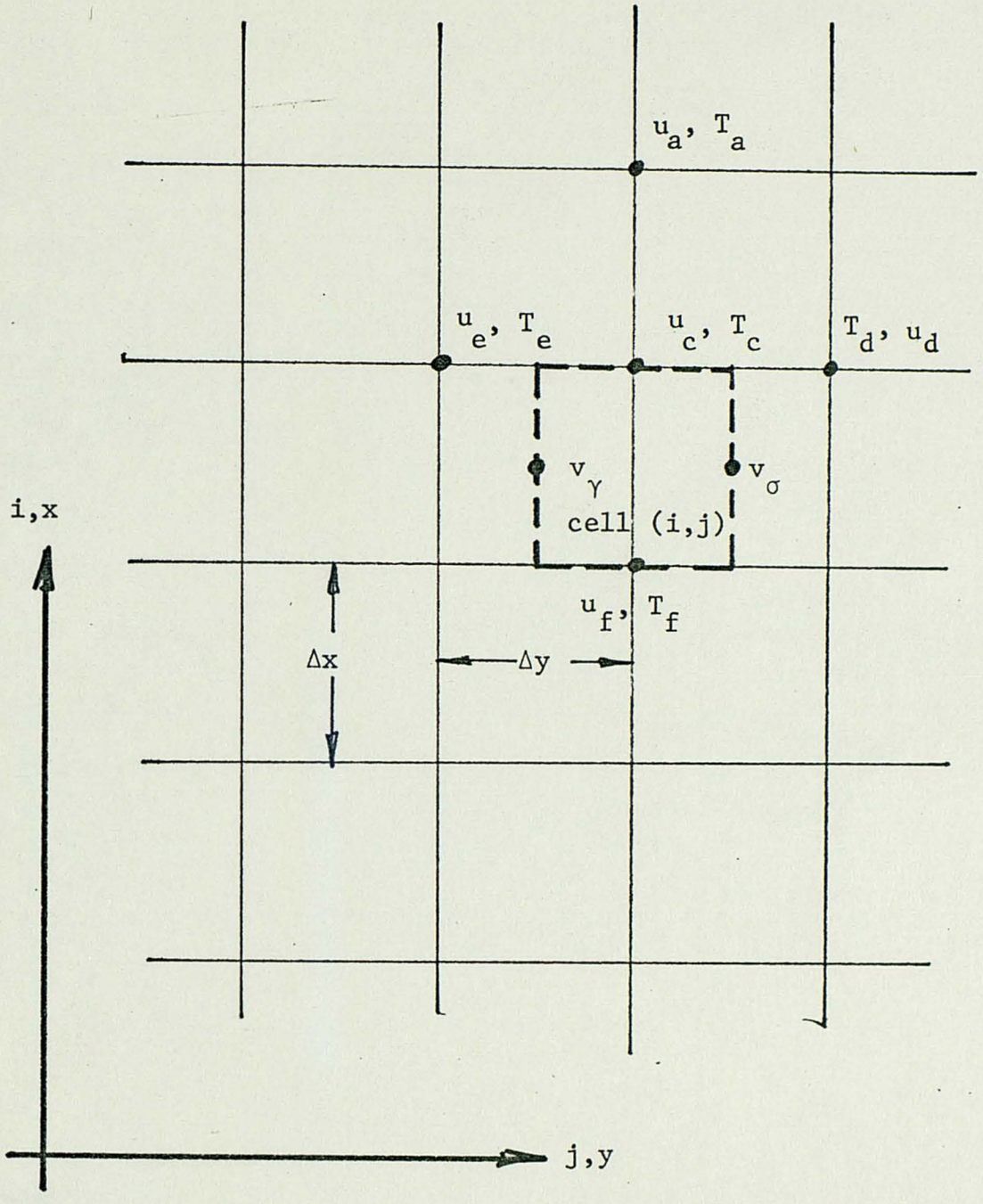

where:

subscript	location
a	(i+1,j)
c	(i,j)
d	(i,j+1)
e	(i,j-1)
γ	(i,j-1)
σ	(i,j)

Fig. 6.--The Computational Grid

calculation. Both the computational procedure and the physical constraints of the problem are identical for either flow case.

Having determined the velocity distribution within the plume, equations (2.40) and (2.41) along with the imposed gradient linearity form the determinate systems from which the temperature distribution is calculated. The computational procedure here is identical with that for the flow problem.

It should be noted here that the computational cells are squares, i.e. $\Delta x = \Delta y$. While this is not a necessary constraint, it does keep the computational procedure simple.

To facilitate the implementation of the computational procedures as outlined above, use is made of an IBM 360 digital computer. A complete program listing and input data format coding is presented in Appendix B.

CHAPTER 3

MODEL VERIFICATION

3.1 Introduction

In the ideal research situation the most rigorous and illuminating test of an analytical model is the comparison of its predictions with actual field data. Where physical limitations of time and money prohibit the implementation of such a study, model verification is reduced to either a comparison of results with the results of a previously verified model, or, where a standard of comparison is lacking, an estimation of the validity of the results based upon a knowledge of what seems reasonable in light of the physics involved, or both.

Because an exhaustive field verification of the model presented here is well beyond the scope of this study, the basis for evaluating its results is the classical two-dimensional momentum jet. By recognizing the physical differences between the two problems an estimation may be made as to whether or not the theoretical results presented appear reasonable.

3.2 Verification of the Flow Model

The essential difference between the classical two-dimensional jet and the problem at hand is the inclusion of the effect of bottom friction in the equation of momentum conservation (equation 2.1). It will be recalled that in section 2.2.1 of Chapter 2 the shearing stress

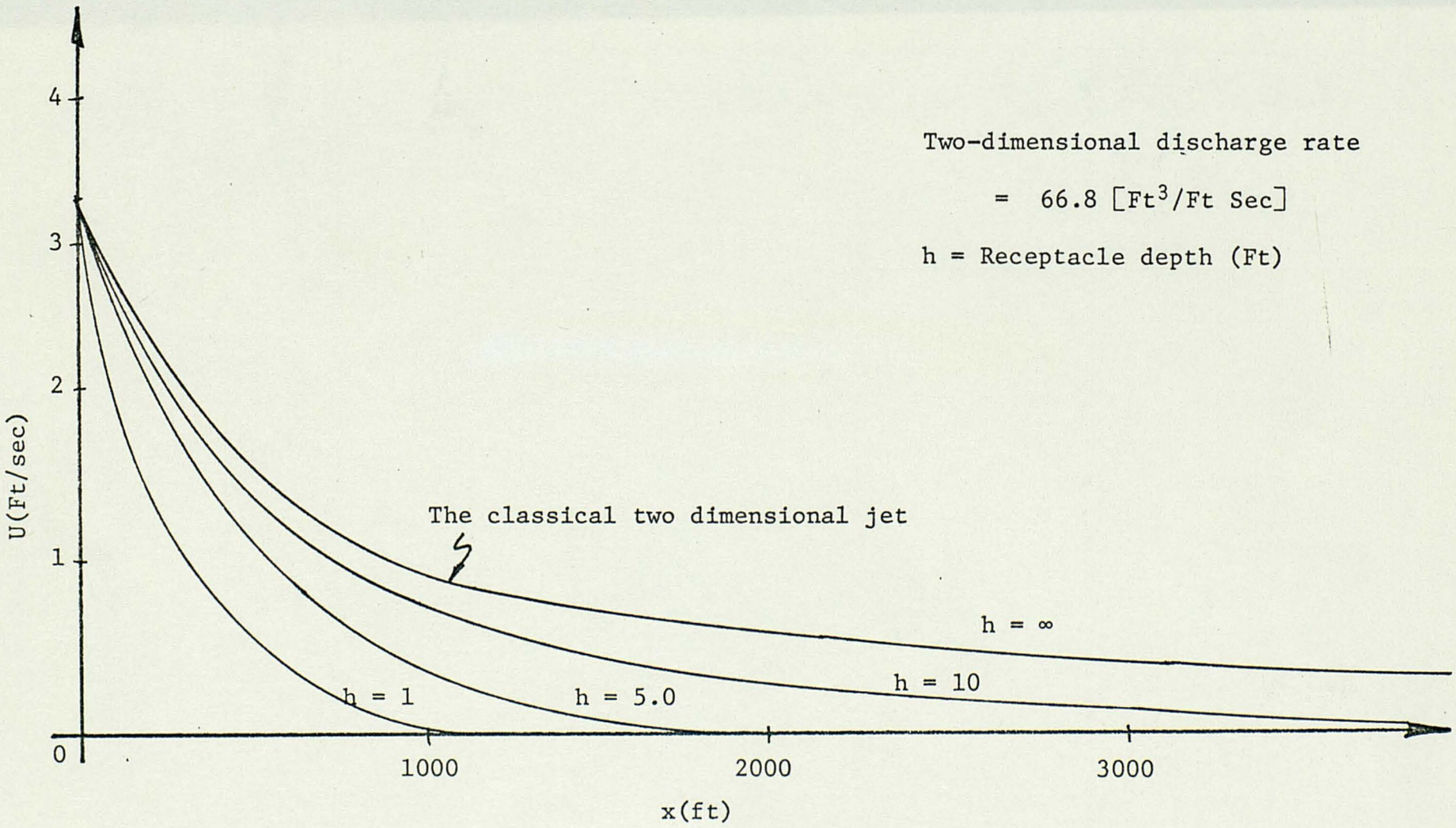

Fig. 7.--The Theoretical Centerline Velocity Distribution

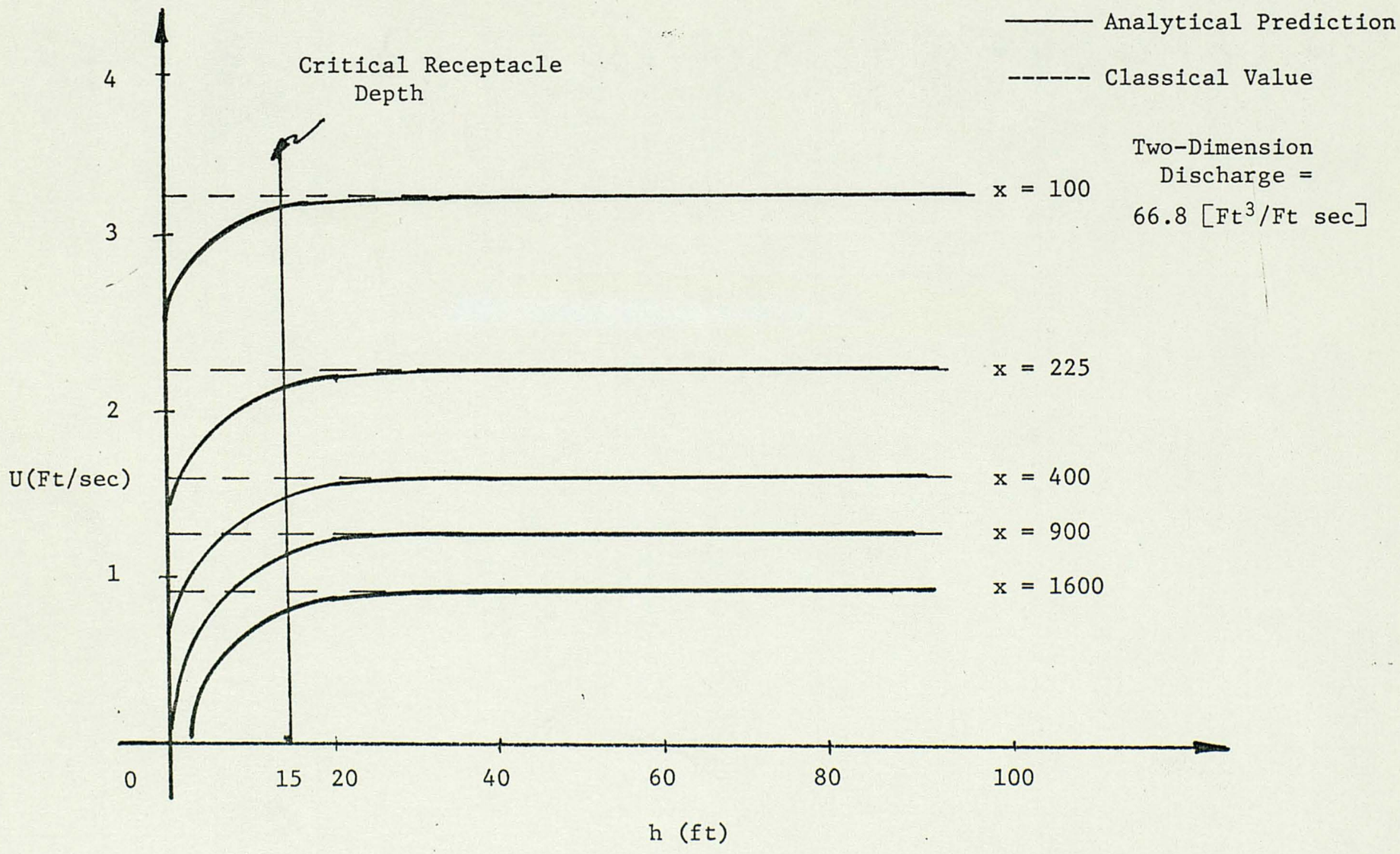

Fig. 8.--The Effect of the Receptacle Depth On The Centerline Velocity

at the receptacle floor was averaged over the depth. Consequently, the effect of bottom friction on the fluid motion of the plume is expected to decrease with increasing receptacle depth. Indeed, the velocity distribution predicted by the model should be identical with that for the classical jet where the receptacle depth is infinite. Furthermore, because both the classical jet and the analytical model presented here assume a Gaussian spanwise velocity distribution, it is necessary to consider only the centerline velocity distributions to determine the relative differences between the two predictions. Figure 7 represents the analytical centerline velocity distribution and shows the effect of bottom friction for various receptacle depths.

As expected, where the receptacle is deep, i.e. as $h \to \infty$, the velocity distribution approaches that for the classical jet, while at shallower depths the deviation from the classical jet becomes more pronounced. This points to the conclusion that there must be some critical receptacle depth, for a given set of effluent conditions, where the flow cannot be reasonably approximated by the classical problem. In other words, for each set of effluent conditions, there is some receptacle depth.for which the effect of bottom friction on the fluid motion in the plume requires that the classical solution be abandoned. Figure 8 shows the theoretical effect of receptacle depth on the centerline velocity over a range of points fixed along the jet axis. In each case the velocity is characteristically asymptotic to the classical prediction and falls off rapidly as $h \to 0$. For the jet configuration considered, that is; for an effluent flow rate of

$66.8\left[\frac{Ft.^3}{Ft.\text{-}Sec.}\right]$, the critical receptacle depth appears to be about fifteen feet.

In order to eliminate the assumptions made in the analytical solution of the flow problem, a numerical analysis, as presented in sections 2.4.1 and 2.4.3 of Chapter 2, was performed. The essential differences between the numerical and analytical solutions are the Gaussian velocity distribution and the empirical jet width relationship, equation (2.19), employed by the analytical solution. In place of these approximations the numerical solution employs a piecewise linear representation for the velocity field. In addition, the numerical solution allows the flow to make the transition from turbulent to laminar, theoretically making the numerical results more compatible with physical reality than the analytical.

Figure 9 depicts the Gaussian velocity distribution of the analytical solution along with the predicted spanwise distribution of the numerical analysis. The two curves agree to within about five percent based upon a least squares deviation.

Figure 10 shows the relationship between the numerically predicted jet width, b, and the downstream distance from the orifice, x, as a function of the receptacle height h. It is noteworthy that the characteristic linear relationship demonstrated for the classical problem appears to have retained its integrity in the numerical solution although, as expected, the value of the constant changes where the effect of bottom friction becomes significant to the flow.

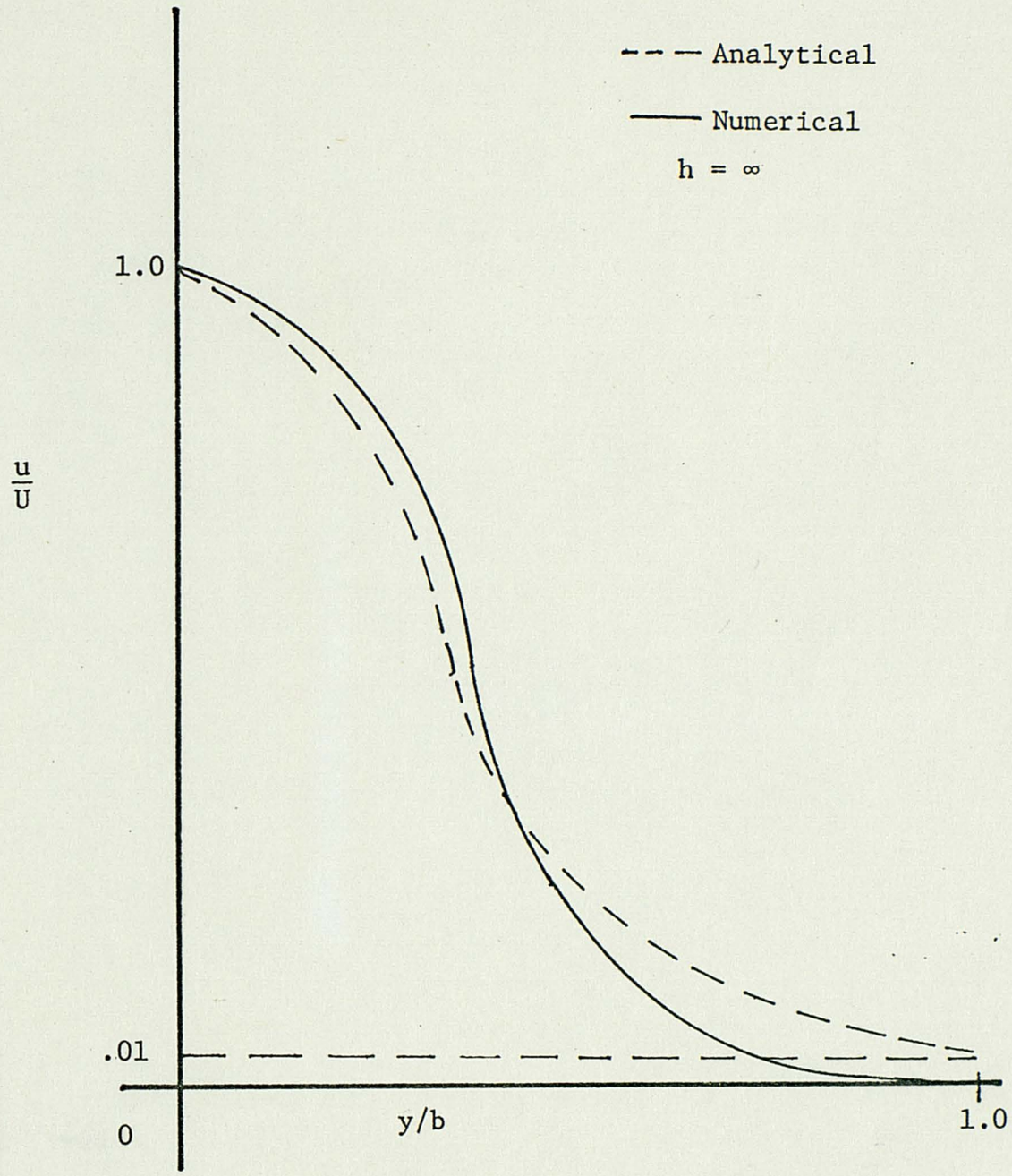

Fig. 9.--Comparison Of The Analytical And Numerical Spanwise Velocity Profiles

Two-dimensional Flow Rate = 66.8 $\frac{Ft^2}{sec}$ (Ft^3/Ft.Sec)

h = receptacle height (Ft.)

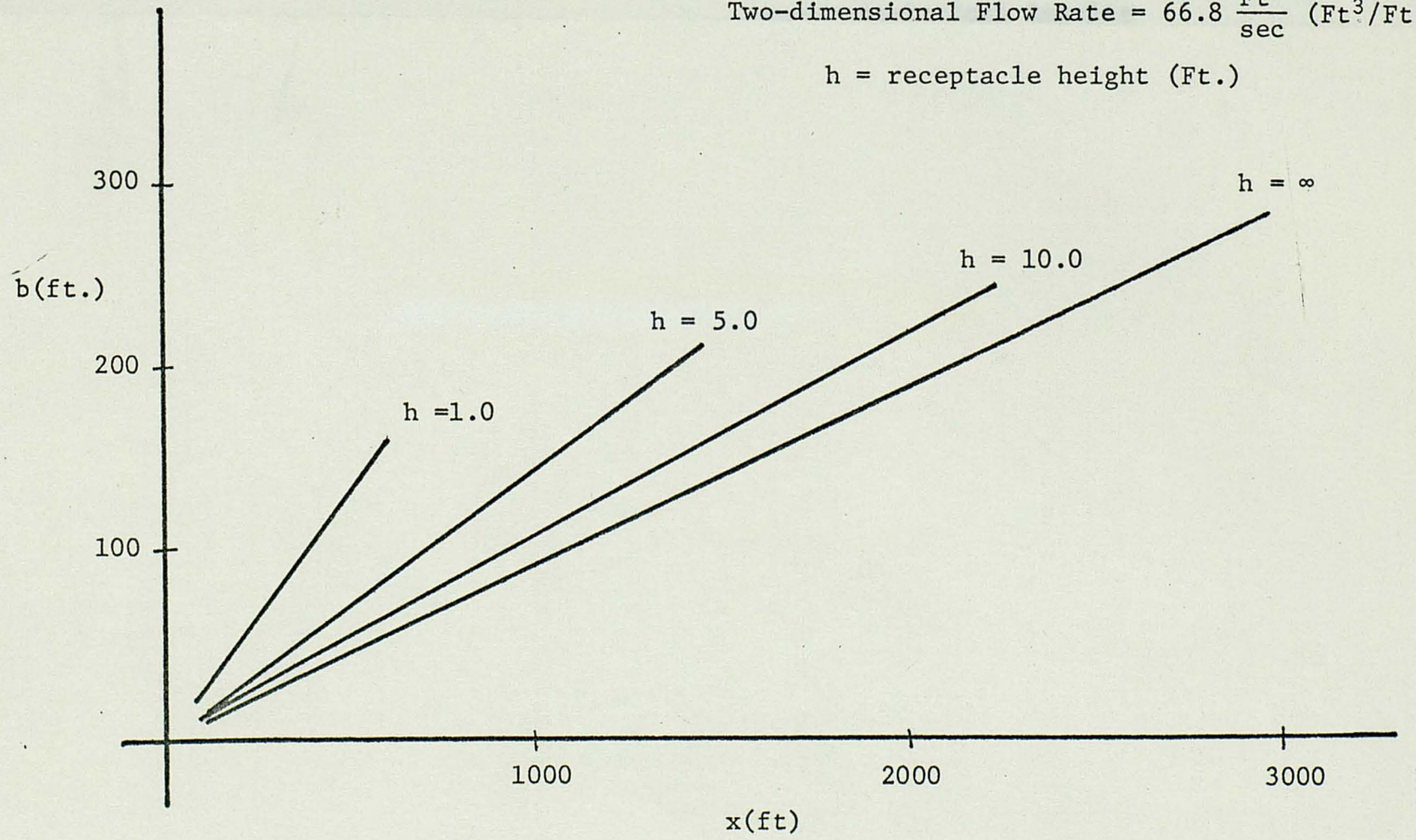

Fig. 10.--The Spreading Of The Jet As Predicted Numerically

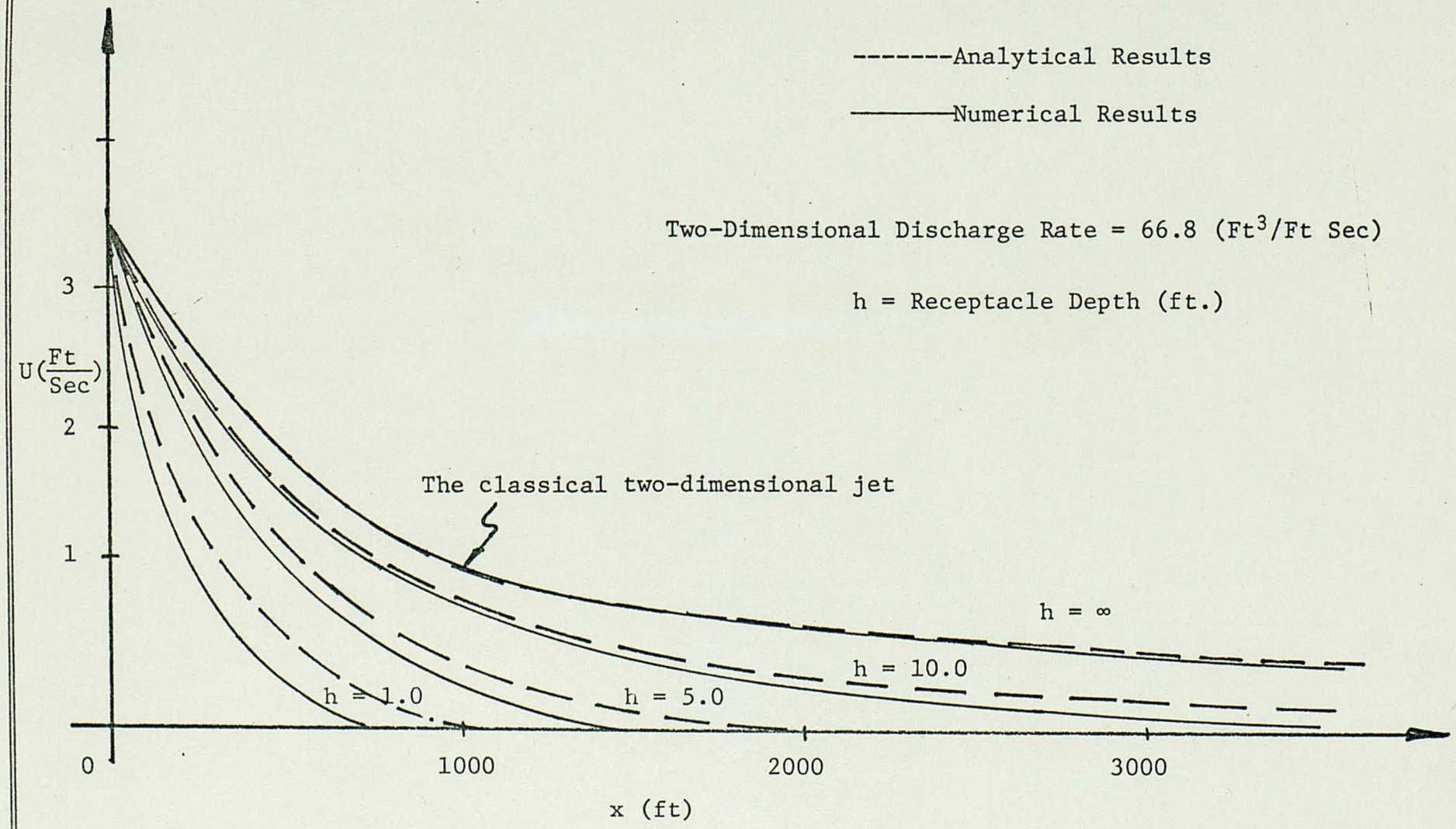

Fig. 11.--Comparison Of The Analytical And Numerical Results For The Centerline Velocity Distribution

Figure 11 shows how the numerical prediction of the centerline velocity compares with the analytical. As expected, the numerical results differ somewhat from the analytical. Again, this is probably due to the fact that the numerical solution allows for flow transition from turbulent to laminar while the analytical does not and that there are fundamental differences in the assumptions used for each solution.

In an attempt to determine the effect of computational grid size on the numerical results, the grid size was varied over a series of computer runs for a range of values from one to ten square feet. The effect on the calculated velocity distribution was virtually non-existant. Most likely this is due to the fact that the grid size was not allowed to exceed half the orifice width, thereby being limited to relatively small dimensions.

3.3 Verification of the Temperature Model

Here again, because the complete two-dimensional analytical temperature distribution is taken to be defined by an empirically demonstrated relationship, equation (2.29), for the classical jet, the crux of the thermal analysis centers about the validity of the center-line temperature distribution as presented by equation (2.36). Figure 12 makes the comparison of the classical results with those obtained from the solution of equation (2.36).

Because conductivity in the downstream jet direction is neglected by the analysis, the expected temperature decrease in the same direction would ordinarily be similar with that for the center-line velocity. However, due to the natural environmental energy exchange discussed in sections 2.3.1 and 2.3.2 of Chapter 2, the temperature decrease is seen to be somewhat more pronounced. In order to eliminate the approximation of equation (2.29) from the analytical solution of the temperature problem the numerical analysis of sections 2.4.2 and 2.4.3 was performed. A comparison of the classical distributions and that resulting from the numerical analysis is presented in Figures 13 and 14.

As with the flow problem, there are deviations here from the analytical solutions. Again, it may be attributed to the ability of the numerical solution to allow the flow transition.

3.4 Extension of the Model

Because the results of the analysis presented for the case of an infinitely deep receptacle are in good agreement with the classical

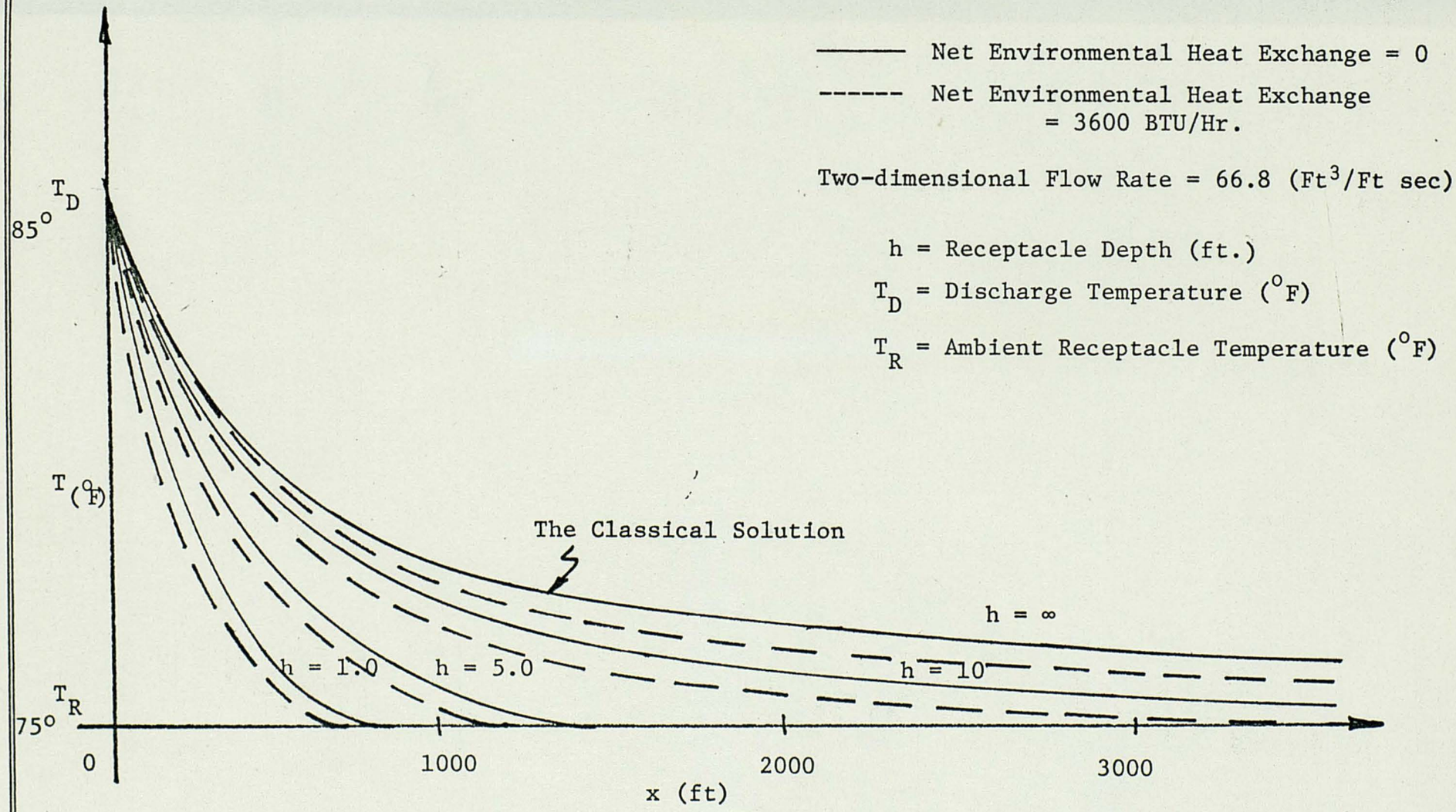

Fig. 12.--The Analytical Centerline Temperature Distribution

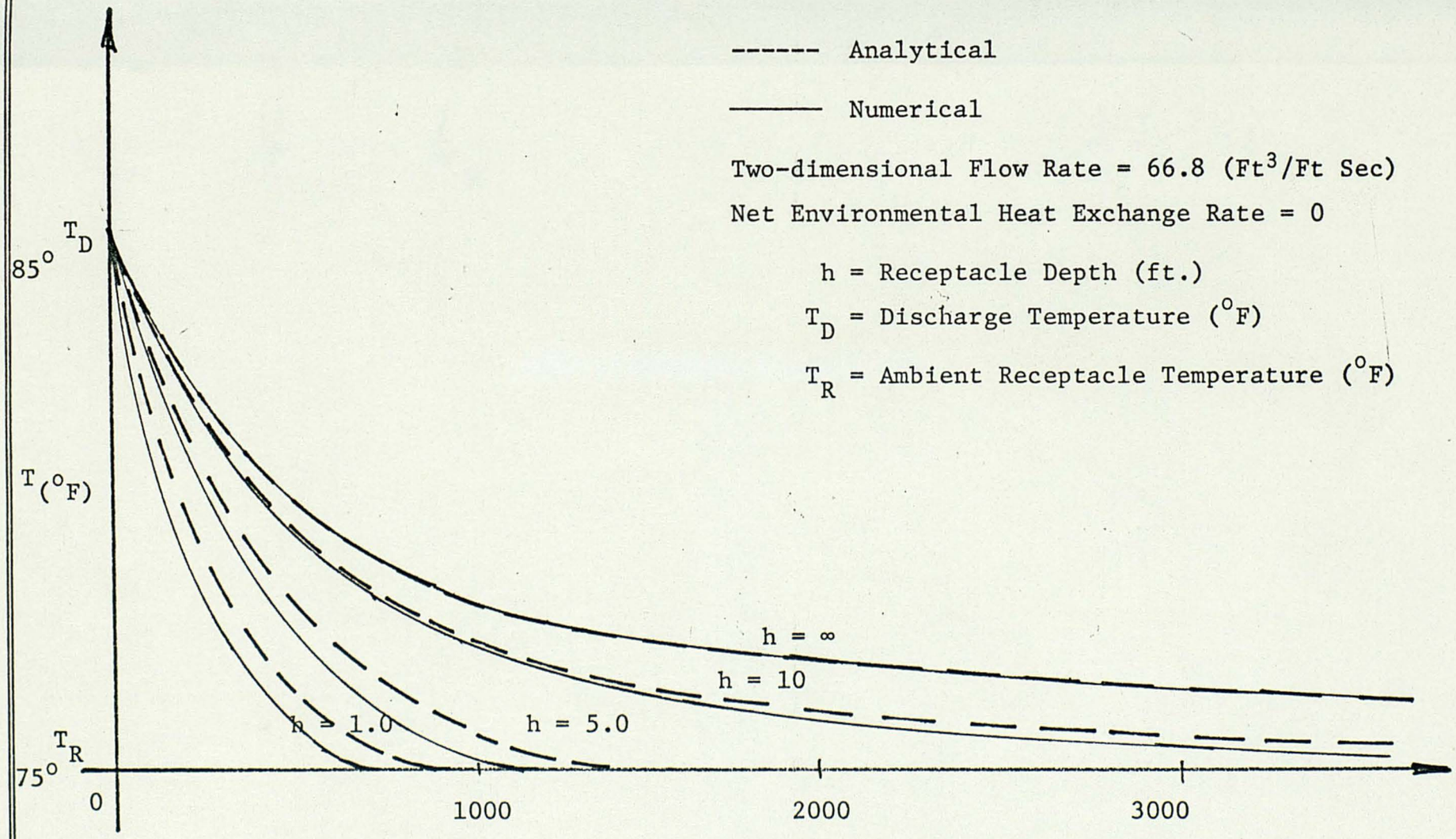

Fig. 13.--Comparison Of The Analytical And Numerical Centerline Temperature Distributions

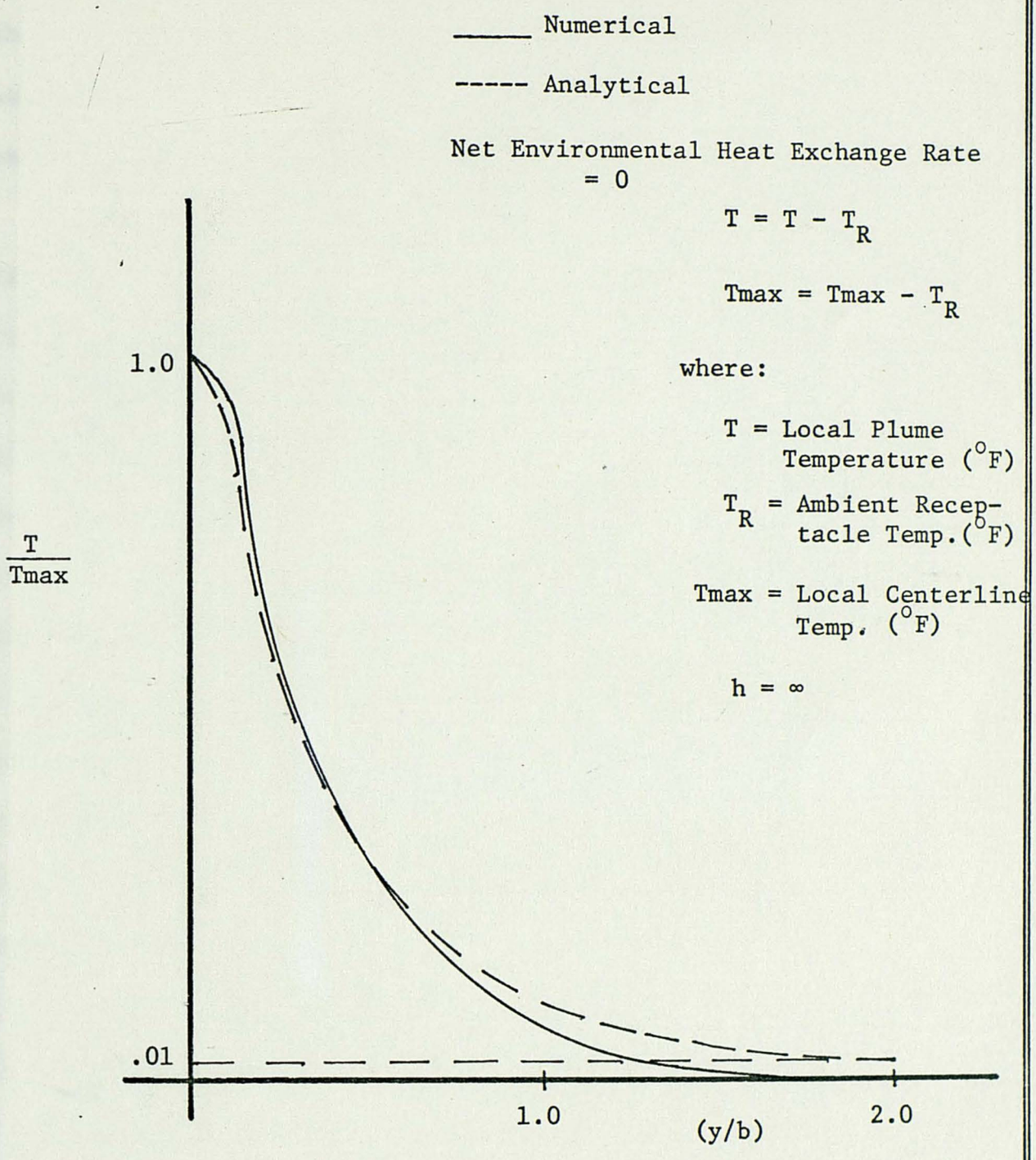

Fig. 14.--The Spanwise Temperature Distributions

results, and because results for shallower receptacles appear reasonable, it would appear that an extension of the model to the case of a non-quiescent receptacle could be made with some success. Such an extension would greatly increase the applicability of the model.

As was seen in Chapter 2, if the two-dimensional velocity distribution generated in the receptacle can be explicitly defined, it is a relatively simple matter to apply that distribution to the energy equation and, with aid of equation (2.29), solve for the complete two-dimensional temperature distribution. At first glance it would appear that a direct vectorial addition of the ambient distribution in the receptacle to equation (2.23) would provide the solution. However, it must be remembered that the equation of momentum conservation, from which equation (2.23) was derived, is non-linear. The principal of direct superposition is therefore not applicable. Itis because of this non-linearity that any attempt at an analytical solution of the problem for the non-quiescent receptacle condition will meet with great difficulty.

On the other hand, because the finite differenced form of the momentum equation is linear within each finite fluid element, it would be possible to superimpose velocities at each nodal point in the computational grid starting at the jet boundary.

In this manner the complete two-dimensional velocity distribution for the condition of a non-quiescent receptacle may be calculated. Having the flow distribution, the temperature distribution would be determined in precisely the same manner as indicated in section 2.4.3.

CHAPTER 4

CONCLUSIONS AND RECOMMENDATIONS

4.1

Comparison of the results of the numerical analysis, as presented in section 2.4 of Chapter 2, with the classical two-dimensional jet indicates that the analysis gives a reasonably good picture of the temperature distribution for a receptacle depth of $h = \infty$ (Figures 13 and 14). Comparison of the numerical results with results from the analytical solution for more shallow receptacle depths also correlate quite well once the realization of flow transition is made and compensated for in the analytical results. The conclusion to be drawn here is that the problem of determining the temperature distribution in a shallow, quiescent receptacle is adequately described by the mathematical model presented in sections 2.2.1 and 2.3.1 of Chapter 2.

4.2

As indicated in Chapter 3, there is a critical dependence of the flow velocity in the plume on the receptacle depth, h (Figure 8). For each set of flow outfall conditions there is a critical receptacle depth above which the classical two-dimensional momentum equation is no longer applicable. It would therefore seem desirable to have a general relationship between this critical depth and the plume outfall conditions. Such a relationship could be generated from equation (2.22) with the criterion of the velocity being equal to some arbitrary fraction of the classical prediction determining the critical depth.

4.3

In order to make the analytical solution to the problem more compatible with physical reality, it is recommended that the incorporation of the effects of flow transition into the analytical model be made. This can be accomplished by the use of the momentum and energy equations for the case of laminar flow where the flow Reynolds number is less than the critical Reynolds Number for flow transition.

4.4

As suggested in Chapter 2, the use of the semi-empirical relationship (equation 2.19) demonstrated for the classical problem in the analytical solution is theoretically unnecessary. While it is true that great difficulties can be foreseen as far as the resulting mathematical manipulations are concerned, some attempt should be made at arriving at a solution to equation (2.17) without the use of equation (2.19).

4.5

While it is true that the results of the analysis compare favorably with established theory, the acid test of any analysis is verfication through empirical correlation. It is therefore reommended that the model be tested through comparison with actual field data. It should be noted that good agreement with field data can exist only if the model is tested where the physical limitations of the analysis are realized.

4.6

In order to extend the general applicability of the model, it is recommended that the incorporation of the effects of a non-quiescent receptacle in the numerical analysis be examined along the lines presented in section 3.3 of Chapter 3. This would involve the node by node velocity superposition detailed in Chapter 3.

APPENDIX A

Intermediate Mathematics Involved In The Analytical Solution Of The Flow Problem

Intermediate Mathematics Involved In The Analytical Solution of The Flow Problem

The following mathematical manipulations follow the development of the flow problem from equation (2.1) through equations (2.17) and (2.18) as presented in section (2.22) of the text.

Momentum equation:

$$u \frac{\partial u}{\partial x} + v \frac{\partial u}{\partial y} = (g_c/\rho)\left[\frac{\partial \tau}{\partial y}\right] - (g_c/\rho)\left[\frac{\tau_b}{h}\right]; \qquad (2.1$$

Continuity:

$$\frac{\partial u}{\partial x} + \frac{\partial v}{\partial y} = 0 ; \qquad (2.2)$$

Consider the left hand side of equation (2.1), i.e.:

$$u \frac{\partial u}{\partial x} + v \frac{\partial u}{\partial y}$$

Integrating over y:

$$\int_0^\infty u \frac{\partial u}{\partial x}\, dy + \int_0^\infty v \frac{\partial u}{\partial y}\, dy = \int_0^b u \frac{\partial u}{\partial x}\, dy + \int_b^\infty u \frac{\partial u}{\partial x}\, dy \quad 1$$

$$+ \int_0^b v \frac{\partial u}{\partial y}\, dy + \int_b^\infty v \frac{\partial u}{\partial y}\, dy \quad 2$$

where:

b = Jet half-width

Note;

$$u(\infty) = u(b) = 0$$

Consider term 1

$$\int_b^\infty u \frac{\partial u}{\partial x}\, dy = 0$$

Because:

$$u(y) = 0 \; ; \; b \leq y < \infty$$

so that:

$$\int_0^\infty u \frac{\partial u}{\partial x} \, dy = \int_0^b u \frac{\partial u}{\partial x} \, dy$$

Now consider term 2

$$\int_0^b v \frac{\partial u}{\partial y} \, dy + \int_b^\infty v \frac{\partial u}{\partial y} \, dy$$

Now:

$$\int_b^\infty v \frac{\partial u}{\partial y} \, dy = \int_b^\infty vdn = uv \Big|_b^\infty - \int_b^\infty u \frac{\partial v}{\partial y} \, dy$$

Recall:

$$u(y) = 0 \; ; \; b \leq y < \infty$$

so that:

$$\int_b^\infty v \frac{\partial u}{\partial y} \, dy = - \int_b^\infty u \frac{\partial v}{\partial y} \, dy = 0$$

Now:

$$\int_0^b v \frac{\partial u}{\partial y} \, dy = uv \Big|_0^b - \int_0^b u \frac{\partial v}{\partial y} \, dy$$

But:

$$uv \Big|_0^b = u(b) \, v(b) - u(0) \, v(0)$$

$$= 0 \cdot v(b) - u(0) \cdot 0 = 0$$

so that:

$$\int_0^b v \frac{\partial u}{\partial y} \, dy = - \int_0^b u \frac{\partial v}{\partial y} \, dy$$

From equation (2.2) (i.e. continuity)

$$\frac{\partial v}{\partial y} = - \frac{\partial u}{\partial x}$$

so that:

$$\int_0^b v \frac{\partial u}{\partial y} dy = \int_0^b u \frac{\partial u}{\partial x} dy$$

and finally, the integral form of equation (2.1) (the left hand side) becomes:

$$\int_0^\infty \left[u \frac{\partial u}{\partial x} + v \frac{\partial u}{\partial y} \right] dy = 2 \int_0^b u \frac{\partial u}{\partial x} dy$$

Now consider the right hand side of equation (2.1) (i.e.)

$$(g_c/\rho) \frac{\partial \tau}{\partial y} - (g_c/\rho) \frac{\tau_b}{h}$$

Two cases must be considered here:

1. Turbulent Flow
2. Laminar Flow

For the turbulent case:

$$\tau = \frac{\rho K b}{g_c} (U - u) \frac{\partial u}{\partial y} \text{ ; side shear} \qquad (2.11)$$

$$\tau_b = \frac{\rho u^2 (.074)}{2 g_c R^{1/5}} \text{ ; bottom shear} \qquad (2.12)$$

so that:

$$\frac{\partial \tau}{\partial y} = \frac{\partial}{\partial y} \left[\rho K b (U - u) \frac{\partial u}{\partial y} \right]$$

where:

$$U = U(x)$$

$$u = u(x, y)$$

and:

$$\frac{\partial \tau}{\partial y} = \frac{\rho Kb}{g_c}\left[U\frac{\partial^2 u}{\partial y2} - U\frac{\partial^2 u}{\partial y2} - \left(\frac{\partial u}{\partial y}\right)^2\right]$$

so that the first term of the right hand side of equation (2.1), for the turbulent case, becomes:

$$(g_c/\rho)\frac{\partial \tau}{\partial y} = Kb\left[\frac{\partial^2 u}{\partial y^2}(U - u) - \left(\frac{\partial u}{\partial y}\right)^2\right]$$

Now consider the second term of the right hand side of equation (2.1) (i.e.,)

$$(g_c/\rho)\ \frac{\tau_b}{h}$$

Recall:

$$\tau_b = \frac{\rho u^2(.074)}{\left[2g_c\right]\left[\frac{\rho ux}{\mu}\right]^{1/5}}$$

so that the integral form of the momentum equation (2.1), for the turbulent case, becomes:

$$2\int_0^b u\frac{\partial u}{\partial x}\,dy = Kb\int_0^b\left[\frac{\partial^2 u}{\partial y^2}(U - u) - \left(\frac{\partial u}{\partial y}\right)^2\right]dy$$

$$-\frac{.037}{h}\int_0^b \frac{u^2}{\left[\frac{\rho ux}{\mu}\right]^{1/5}}\,dy\ ; \qquad (2.13) \text{ and } (2.8)$$

Following the above procedure for the laminar case, except making the substitutions of equations (2.9) and (2.10) rather than (2.11) and (2.12) yields:

$$2\int_0^b u\frac{\partial u}{\partial x}\,dy = \frac{\mu}{\rho}\int_0^b \frac{\partial^2 u}{\partial y^2}\,dy + \frac{.332}{h}\int_0^b -\frac{u^2}{\left[\frac{\rho ux}{\mu}\right]^{\frac{1}{2}}}\,dy\ ; \qquad (2.14) \text{ and } (2.8)$$

In order to integrate the above equations over y, a Gaussian velocity distribution is assumed as shown in Figure 3.

so that:

$$\frac{u}{U} = e^{-4.606(y/b)^2} \quad ; \; U = U(x)$$

$$u = u(x, y)$$

and:

$$u = Ue^{-4.606(y/b)^2}$$

$$u^2 = U^2e^{-9.212(y/b)^2}$$

$$\frac{\partial u}{\partial y} = -\, 9.212\; y/b^2\; Ue^{-4.606(y/b)^2}$$

$$\left(\frac{\partial u}{\partial y}\right)^2 = 84.86\; (y/b^2)^2\; U^2e^{-9.212(y/b)^2}$$

$$\frac{\partial^2 u}{\partial y^2} = 84.86\; (y/b^2)^2\; Ue^{-4.606(y/b)^2} - \frac{9.212}{b^2}\; Ue^{-4.606(y/b)^2}$$

Substituting for

$$u,\; u^2,\; \frac{\partial u}{\partial y},\; \left(\frac{\partial u}{\partial y}\right)^2,\; \text{and}\; \frac{\partial^2 u}{\partial y^2}$$

in the integral form of the momentum equation (for the turbulent case) yields:

[1]

$$\frac{-4(4.606)}{C^2}\; U^3\; \frac{dU}{dx} \int_0^b y^2 e^{-2(4.606)y^2U^2/c^2} dy + 2U\; \frac{dU}{dx} \int_0^b e^{-2(4.606)y^2U^2/c^2}$$

$$= Kb \int_0^b \left[84.86(y/b^2)^2\; Ue^{-4.606(y/b)^2} - \frac{9.212}{b^2}\; Ue^{-4.606(y/b)^2}\right. \quad [2]$$

$$\left. U - Ue^{-4.606(y/b)^2} - 84.86(y/b^2)^2\; U^2e^{-9.212(y/b)^2}\right] dy$$

$$-\frac{.037}{h}\int_0^b \frac{U^2 e^{-9.212(y/b)^2}}{\left[\frac{\rho U e^{-4.606(y/b)^2}\, x}{\mu}\right]^{1/5}}\, dy\ ; \qquad [3]$$

(2.16)

where:

$$C = 2.84\ U(0)\ b(0)$$

Recalling that U = U(x) only and integrating the left hand side of the above equation, yields:

$$\frac{-4(4.606)}{C^2}\ U^3\ \frac{dU}{dx}\int_0^b y^2 e^{-2(4.606)y^2U^2/C^2} dy$$

$$+\ 2U\ \frac{dU}{dx}\int_0^b e^{-2(4.606)y^2U^2/C^2}\ dy$$

$$= Ub\frac{dU}{dx}\ e^{-2(4.606)U^2/C^2} + \frac{.75C}{U\sqrt{9.212}}$$

From the equation of conservation of mass it will be recalled that

$$b = \frac{C}{U}$$

so that the left hand side of the momentum equation becomes:

$$C\ \frac{dU}{dx}\ e^{-2(4.606)U^2/C^2} + \frac{.75C^2}{\sqrt{2(4.606)}}\ \frac{1}{U}\ \frac{dU}{dx}$$

Now consider term [2] of the integral form of the momentum equation for the turbulent case i.e.;

$$Kb \int_0^b \{84.86\ (y/b^2)^2\ U^2 e^{-4.606(y/b)^2} \qquad [a]$$

$$-9.212\ \frac{U^2}{b^2}\ e^{-4.606(y/b)^2} \qquad [b]$$

$$+9.212 \frac{U^2}{b^2}\ e^{-9.212(y/b)^2} \qquad [c]$$

$$-169.72\ (y/b^2)\ \ U^2 e^{-9.212(y/b)^2}\ \}dy \qquad [d]$$

Consider term [a] of the above expression

$$[a] = \int_0^1 84.86\ (y/b^2)\ \ U^2\ \frac{b^2}{2y}\ e^{-4.606(y/b)^2}\ d[(y/b)^2]$$

$$= 42.43\ \frac{U^2}{b} \int_0^1 (y/b)\ e^{-4.606(y/b)^2}\ d[(y/b)^2]$$

$$= C \int_0^1 \sqrt{x}\ e^{ax}\ dx\ ;\quad C = 42.43\ \frac{U^2}{b}$$

$$a = -4.606$$

$$x = (y/b)^2$$

Integrating by parts with

$$u = \sqrt{x} \qquad dv = e^{ax}\,dx$$

$$du = \tfrac{1}{2}x^{-\frac{1}{2}}\,dx \qquad v = \frac{e^{ax}}{a}$$

$$I = C\left[\frac{\sqrt{x}\,e^{ax}}{a}\Big|_0^1 - \int_0^1 \frac{e^{ax}}{2a\sqrt{x}}\,dx\right]$$

$$= C\left[\frac{e^a}{a} - \frac{1}{2a}\int_0^1 \frac{1}{\sqrt{x}}\,e^{ax}\,dx\right]$$

$$= C\left[\frac{e^a}{a} - \frac{1}{2a}\left(\frac{1.5}{\sqrt{-a}}\right)\right]$$

so that:

$$[a] = 42.43\,\frac{U^2}{b}\left[\frac{e^{-4.606}}{-4.606} + \left(\frac{1}{2(4.606)}\right)\left(\frac{1.5}{4.606}\right)\right]$$

and finally:

$$[a] = 3.1719\,\frac{U^2}{b}$$

Now consider term [b]

$$[b] = \int_0^b -9.212\,\frac{U^2}{b^2}\,e^{-4.606(y/b)^2}\,dy$$

$$= \int_0^1 -9.212\,\frac{U^2}{b^2}\,\frac{b^2}{2y}\,e^{-4.696(y/b)^2}\,d[(y/b)^2]$$

$$= -4.606\,\frac{U^2}{b}\int_0^1 (b/y)\,C^{-4.606(y/b)^2}\,d[(y/b)^2]$$

$$= C\int_0^1 \frac{1}{\sqrt{x}}\,e^{ax}\,dx \;;\quad C = -\frac{4.606\,U^2}{b}$$

$$a = 4.606$$

$$x = (y/b)^2$$

$$b = C \frac{2}{\sqrt{-a}} [.75]$$

and finally:

$$b = - 3.2192 \frac{U^2}{b}$$

Now consider term [c]

$$[c] = \int_0^b 9.212 \frac{U^2}{b^2} e^{-9.212(y/b)^2} dy$$

$$= 9.212 U^2 \int_0^1 \frac{b^2}{2yb^2} e^{-9.212(y/b)^2} d[(y/b)^2]$$

$$= 4.606 \frac{U^2}{b} \int_0^1 \left(\frac{b}{y}\right) e^{-9.212(y/b)^2} d[(y/b)^2]$$

$$= 4.606 \frac{U^2}{b} \frac{2}{\sqrt{9.212}} (.75)$$

and finally

$$[c] = 2.2766 \frac{U^2}{b}$$

Now consider term [d]

$$[d] = \int_0^b - 169.72 (y/b^2)^2 U^2 e^{-9.212(y/b)^2} dy$$

$$= - 84.86 \frac{U^2}{b} \int_0^1 (y/b) e^{-9.212(y/b)^2} d[(y/b)^2]$$

$$[d] = - 84.86 \frac{U^2}{b} \left[\frac{e^{-9.212}}{-9.212} + \frac{1}{2(9.212)} \frac{1.5}{\sqrt{9.212}} \right]$$

and finally

$$[d] = - 2.2766 \frac{U^2}{b}$$

Recalling that term [2] of the integral form of the momentum equation, for the turbulent case is

$$[2] = Kb\,\{[a] + [b] + [c] + [d]\}$$

$$[2] = Kb\,\frac{U^2}{b}\,[3.1719 - 3.2192 + 2.2766 - 2.2766]$$

$$[2] = -\ .0473\ K\ U^2$$

Now consider term [3] of the integral form of the momentum equation for the turbulent case, i.e.,

$$[3] = \frac{.037}{h}\int_0^b \frac{U^2\ e^{-9.212(y/b)^2}}{\left[\frac{\rho U e^{-4.606(y/b)^2}\ x}{\mu}\right]^{1/5}}\ dy$$

$$= \frac{.037\ U^2}{h\left[\frac{\rho U x}{\mu}\right]^{1/5}}\int_0^b \frac{e^{-9.212(y/b)^2}}{e^{-.9212(y/b)^2}}\ dy$$

$$[3] = \frac{.0185\ U^2 b}{h\left[\frac{\rho U x}{\mu}\right]^{1/5}}\int_0^1 \left(\frac{b}{y}\right)\ e^{-8.291(y/b)^2}\ d[(y/b)^2]$$

$$= \frac{.0185\ U^2 b}{h\left[\frac{\rho U x}{\mu}\right]^{1/5}}\ \frac{1.5}{\sqrt{8.291}}$$

and finally

$$[3] = \frac{.00925\ U^2 b}{h\left[\frac{\rho U x}{\mu}\right]^{1/5}}$$

so that the integrated form of the momentum equation for the turbulent case is

$$C\frac{dU}{dx}e^{-2(4.606)U^2/C^2} + \frac{.75C^2}{\sqrt{9.212}}\frac{1}{U}\frac{dU}{dx}$$

$$= -.04KU^2 - \frac{.00925U^2b}{h\left[\frac{\rho Ux}{\mu}\right]^{1/5}}$$

which is identically equation (2.17).

By following the above procedure for the laminar case, the integrated form of the momentum equation becomes:

$$C\frac{dU}{dx}e^{-2(4.606)U^2/C^2} + \frac{.75C^2}{\sqrt{9.212}}\frac{1}{U}\frac{dU}{dx}$$

$$= -.04\frac{\mu}{b\rho} - \frac{.095U\ b}{h\left[\frac{\rho Ux}{\mu}\right]^{\frac{1}{2}}}$$

which is equation (2.18).

APPENDIX B

Computer Program Listing And

Input Data Coding Format

```
C     THE FOLLOWING PROGRAM IS USED TO CALCULATE THE TWO DIM-
                                                ENSIONAL
C     TEMPERATURE DISTRIBUTION FROM A WASTE HEAT OUTFALL. IT-
                                                 IS THE
C     COMPUTATIONAL PROCEDURE USED TO SOLVE THE FINITE DIFFE-
                                                RENCED
C     EQUATIONS OF TWO DIMENSIONAL MOMENTUM AND ENERGY TRANS-
                                                PORT.
C     THE NOTATION FOR THE PROGRAM IS AS FOLLOWS*
C     MU= THE ABSOLUTE VISCOSITY OF THE EFFLUENT
C     NU= THE KINEMATIC VISCOSITY OF THE EFFLUENT
C     CAPA= THE EMPIRICAL CONSTANT IN THE EXPRESSION FOR THE-
                                                VIRTUAL
C     TURBULENT SHEARING STRESS.
C     H= THE RECEPTACLE DEPTH IN FEET
C     DELX AND DELY= THE DIMENSIONS OF THE COMPUTATIONAL CEL-
                                                L
C     ALPHA= THE THERMAL CONDUCTIVITY AT THE ESTIMATED AVERA-
                                                GE PLUME
C     TEMPERATURE
C     RHO= THE DENSITY OF THR EFFLUENT AT THE ESTIMATED AVER-
                                                AGE PLUME
C     TEMPERATURE
C     WS= THE WIND SPEED IN KNOTS
C     P= THE ATMOSPHERIC PRESSURE IN INCHES OF MERCURY
C     QC= THE SUMMATION OF THE HEAT FLUXES RESULTING FROM AD-
                                                VECTION,
C     RADIATION, AND EVAPORATION AS DEFINED IN THE BODY OF T-
                                                HE PAPER
C     TAT= ATMOSPHERIC TEMPERATURE IN DEGREES F
C     B= THE PLUME HALF WIDTH
C     THE PROGRAM BEGINS BY SETTING THE COMPUTATIONAL GRID S-
                                                IZE.
      DIMENSION U(500,25),V(500,25),T(500,25),EPS(4)
      REAL MU
      REAL NU
      DO 111 I=1,500
      DO 111 J=1,25
      V(I,J)=0.0
      V(I,1)=0.
  111 U(I,J)=0.0
C     THE PROGRAM NOW READS THE INPUT DATA.
      READ(5,1000)CAPA,NU,H,RC,DELX,DELY
 1000 FORMAT(6F10.5)
      READ(5,1100)(EPS(I),I=1,4)
 1100 FORMAT(4F10.5)
      READ(5,1300)ALPHA,RHO,WS,P,SP,MU,QC,TAT
```

```
 1300 FORMAT(8F10.5)
      DO 10 I=1,5
   10 READ(5,1200)(U(I,J),J=1,20)
 1200 FORMAT (20F4.0)
      DO 11 I=1,5
   11 READ(5,1400)(T(I,J),J=1,25)
 1400 FORMAT(25F3.0)
C     THE PROGRAM NOW BEGINS CALCULATION OF THE TWO DIMENSIO-
                                                NAL
C     VELOCITY DISTRIBUTION.
      J=2
      I=5
      JP1=2
      KTR=0
      IM1=I-2
   25 IF(U(IM1,JP1).EQ.0.0) GO TO 35
      KTR=KTR+1
      JP1=JP1+2
      GO TO 25
   35 B=(DELY)*KTR
   44 CONTINUE
   42 U(I,1)=U(I,2)
      R=(U(I,J)*((I*(DELX/1))))/NU
      IF(R.LE..1) GO TO 46
      IF(R.LE.RC) GO TO 45
      CF=.074*(1/(R**.2))
      K2=CAPA*B
      A=K2*((U(I,1)-U(I,J))*(U(I,J+1)+U(I,J-1)-2*U(I,J))
     1-(U(I,J+1)-U(I,J-1))**2)/4*(DELY**2)
   50 D=V(I,J-1)*(U(I,J+1)-U(I,J-1))*DELX/DELY*U(I,J)
      C=(U(I-1,J)-U(I,J))*(U(I,J+1)-U(I,J-1))/U(I,J)
      E=U(I,J)*CF*DELX/H
C     THE FOLLOWING EQUATION REPRESENTS THE EQUATION OF MOME-
                                                NTUM
C     CONSERVATION
      U(I+1,J)=U(I-1,J)-E+(DELX/2*U(I,J))*A-D+C
      WRITE(6,2000)I+1,J,U(I+1,J)
 2000 FORMAT(1X,'U(',I3,',',I3,')=',E14.6)
      IF(U(I+1,J).LT.0.0) GO TO 57
      GO TO 55
   45 CF=.664*(1/(R**.5))
   47 A=NU*(U(I,J+1)+U(I,J-1)-2*U(I,J))/4*(DELY**2)
      GO TO 50
   46 CF=0.0
      GO TO 47
C THE PROGRAM NOW CHECKS ON THE LINEARITY OF THE X VELOCITY -
                                                GRADIENT.
   55 TMP=(U(I+1,J)+U(I-1,J))/2
      IF((ABS(TMP-U(I,J))).LE.EPS(1)) GO TO 60
      U(I,J)=ABS(TMP)
```

```
      GO TO 42
   57 U(I+1,J)=0.0
      U(I,J)=U(I+1,J)+U(I-1,J)/2
      GO TO 55
   60 IF(U(I,1)-EPS(2).LE.0)GO TO 411
      V(I,J)=(DELY/DELX)*(U(I,J-1)-U(I,J))+V(I,J-1)
   85 IF((ABS(U(I+1,J))).LE.EPS(3))GO TO 75
      IF(J.GE.24) GO TO 99
      J=J+1
      GO TO 44
   75 IF((ABS(J*(DELY/1)-B)).LE.DELY) GO TO 80
      B=J*DELY
      GO TO 44
   80 FLG=0
      K=J+2
   81 DO 95 M1=K,25
      U(I,M1)=0
   95 V(I,M1)=V(I,J)
      FLG=FLG+1
      IF(FLG-1)96,96,97
   96 I=I-1
      GO TO 81
   97 IF(FLG.EQ.3)GO TO 98
      I=I+2
      GO TO 81
C     THE PROGRAM NOW BEGINS CALCULATION OF TEMPERATURE DIST-
                                              RIBUTION
   98 J=2
      I=I-1
  101 IF(U(I,J).LE.0.0) GO TO 105
  100 T(I,1)=T(I,2)
      R=U(I,J)*I/NU
      IF(R.LE.RC) GO TO 106
      AA=(ALPHA/RHO*SP)*(T(I,J+1)+T(I,J-1)-2*T(I,J))/4.*(DEL-
                                              X**2)
     1+((T(I,J-1)-T(I,J+1))/2*DELY)*K2*U(I,J)
  107 BB=(778.*MU/RHO*SP)*(DELX/U(I,J))*((U(I,J-1)-U(I,J+1))-
                                              **2.)/
     12.*(DELY**2.)
      CC=(V(I,J)*DELX/U(I,J))*(T(I,J+1)-T(I,J-1))/DELY
      DD=(.000558*DELX/(H*RHO*SP*U(I,J)))*(QC-.00407*WS*P*(T-
                                              AT-T(I,J)))
C     THE FOLLOWING EQUATION REPRESENTS THE TWO DIMENSIONAL -
                                              ENERGY
C     EQUATION
      T(I+1,J)=(2*DELX/U(I,J))*AA+BB-CC+DD+T(I-1,J)
      WRITE(6,2500)I+1,J,T(I+1,J)
 2500 FORMAT(1X,'T(',I3,',',I3,')=',E14.6)
C     THE PROGRAM NOW CHECKS ON THE LINEARITY OF THE X TEMPE-
                                              RATURE GRADIENT
```

```
109 PMT=(T(I+1,J)+T(I-1,J))/2.
    IF((ABS(PMT-T(I,J))).LE.EPS(1)) GO TO 120
    T(I,J)=PMT
    GO TO 100
106 AA=(ALPHA/RHO*SP)*(T(I,J+1)+T(I,J-1)-2*T(I,J))/4.*(DEL-
                                                  Y**2.)
    GO TO 107
105 T(I,J)=((ALPHA/RHO*SP)*T(I,J-1))/((ALPHA/RHO)*SP-V(I,J-
                                                  )*DELY)
    IF(T(I,J).GE.T(1,20)) GO TO 112
    T(I,J)=T(1,20)
112 T(I+1,J)=2*T(I,J)-T(I-1,J)
120 J=J+1
    IF(J.LE.24) GO TO 101
    GO TO 99
 99 I=I+1
    J=2
    IF(499-I.LE.0)GO TO 411
    GO TO 44
411 NN=J+1
    DO 500 L=1,I
500 WRITE(6,2000)(L,M,U(L,M),M=1,NN)
    NN=J+2
    DO700 L=1,I
700 WRITE(6,2100)(L,M,T(L,M),M=1,NN)
    STOP
    END
```

INPUT DATA FORMAT CODING

CARDS	COLS.	INPUT QNTY.	PHYSICAL QNTY.	FORMAT
1	1-10	Cappa	K Empirical Constant in Turbulent Shear	F(10.5)
	11-20	Nu	ν Kinematic Viscosity	F(10.5)
	21-30	H	h Receptacle Depth (ft.)	F(10.5)
	31-40	RC	Re_{crit} Transition Reynolds Number	F(10.5)
	41-50	Delx	Δx x-wise cell dimension (ft.)	F(10.5)
	51-60	Dely	Δy y-wise cell dimension (ft.)	F(10.5)
2	1-10	Eps.(1)	Small Numbers	F(10.5)
	11-20	Eps.(2)	Used for comparison	F(10.5)
	21-30	Eps.(3)	Of computed values	F(10.5)
	31-40	Eps.(4)	In Program	F(10.5)
3	1-10	Alpha	α Thermal Conductivity $\left(\frac{BTU}{sec\text{-}Ft\text{-}^{\circ}F}\right)$	F(10.5)
	11-20	Rho	ρ Density of effluent $\frac{lbs.}{Ft^3}$	F(10.5)
	21-30	Ws	V Windspeed (knots)	F(10.5)
	31-40	P	P Atmospheric Pressure	F(10.5)
	41-50	SP	Cp Specific Heat of Effluent	F(10.5)
	51-60	Mu	μ Viscosity $\frac{lbs}{Ft\text{-}sec}$	F(10.5)
	61-70	Qc	Qc Heat flux summation of Advective + Radiative - Evaporative	F(10.5)
4-8	1-80	U	U Velocity of effluent in orifice channel--The number of values input will determine the orifice half width	20 F(4.0)
9-13	1-80	T	T Temperatures of effluent in orifice and ambient receptacle	25 F(3.0)

APPENDIX C

A Summary of Numerical Results

A Summary of Numerical Results

The following tables are a representative sampling of the values used to generate the curves for the numerical centerline and spanwise velocity and temperature distributions presented in Chapter 3. The centerline distributions were taken directly from the calculated values while for the spanwise distributions shown it was necessary to use a certain amount of smoothing of the numerical results. Specifically, in choosing a downstream location at which to depict the spanwise profiles, it was necessary to go far enough into the plume to lose the characteristic step function profile of the outfall channel.

THE CENTERLINE DISTRIBUTIONS FOR:

$T_D = 85^{\circ}F$

Net Environmental Heat Exchange = 0.0

U(0) = 3.34 (Ft./Sec.)

h (ft.)	x (ft.)	U (ft./sec.)	T_{max} $^{\circ}F$
∞	0	3.34	85.0
	500	1.78	81.0
	1000	.98	78.4
	2000	.57	77.0
	3000	.39	76.3
10.0	0	3.34	85.0
	500	1.67	79.7
	1000	.82	77.3
	2000	.31	75.8
	3000	.19	75.5
5.0	0	3.34	85.0
	250	2.23	80.3
	500	1.0	77.7
	1000	.28	75.3
	1500	.10	75.0
1.0	0	3.34	85.0
	200	1.2	78.8
	400	.44	76.6
	600	.20	75.2
	800	0.0	75.0

THE SPANWISE DISTRIBUTIONS FOR:

$T_D = 85^{\circ}F$

Net Environmental Heat Exchange = 0.0

U(0) = 3.34 (Ft./Sec.)

x = 2000 Ft.

h (ft.)	b (ft.)	y (ft.)	u (ft./sec.)	T ($^{\circ}F$)
∞	200	0	.6	77.0
		50	.45	76.2
		100	.15	75.6
		150	.03	75.4
		200	0.0	75.2
		300	0.0	75.1
		400	0.0	75.0

REFERENCES

1. U. S. Department of the Interior, Federal Water Pollution Control Administration, Industrial Waste Guide on Thermal Pollution, Corvallis, Oregon, Northwest Region, Pacific Northwest Water Laboratory, 1968.

2. Remirez, R., "Thermal Pollution -- Hot Issue for Industry," Chemical Engineering, 75: pages 48-50, 1968.

3. Kolflat, T., "Thermal Discharges," Industrial Water Engineering, 5: pages 26-31, 1968.

4. Everts, C. M., "Temperature As A Water Quality Parameter," Water Temperature -- Influences, Effects, and Control, Proceedings of the Twelfth Pacific Northwest Symposium on Water Pollution Research, pages 2-5, Corvallis, Oregon, November, 1963.

5. Hobbs, G. D., "The Mathematical Modelling Of A Stratified Estuary," preprint, presented at the 5th International Water Pollution Research Conference, England, 1970.

6. Dake, J. and Harleman, D., "An Analytical and Experimental Investigation of Thermal Stratification in Lakes and Ponds," Hydrodynamics Report No. 99, Boston, Massachusetts, MIT, 1966.

7. Sawyer, D. N. and McCarty, P., Chemistry for Sanitary Engineers, New York, McGraw-Hill, 1967.

8. Ordal, E. J. and Pacha, R. E., "The Effects of Temperature on Disease in Fish," pages 39-56, (see reference 4).

9. Brett, J. R., "Some Principles in the Thermal Requirements of Fishes," Quarterly Review of Biology, 31: pages 75-87, 1956.

10. U. S. Department of the Interior, Federal Water Pollution Control Administration, Water Quality Criteria, Report of the National Technical Advisory Committee, Washington, D. C., April, 1968.

11. Warner, M., "The Thermal Mixing Zone -- Its Definition," preprint, paper #71-WA/PTC-4, presented at ASME Winter Annual Meeting, Washington, D. C., 1971.

12. McLay, R. W., Hundal, M. S., Martinek, F., and Henson, E. B., "Mathematical Modelling of Nuclear Plant Thermal Effects in Lake Champlain," preprint, paper #71-WA/PWR-4, presented at ASME Winter Annual Meeting, Washington, D. C., 1971.

13. Giles, W., Johnson, N., McComb, G., Morris, F., Schell, Jr., Young, J., "A Thermal Effluent Analysis for Electric Power Generating Plants," Technical Information Series No. 71SD257, Philadelphia, Pennsylvania, Re-entry and Environmental Systems Division, General Electric Company, 1971.

14. Stolzenbach, K. D., and Harleman, D. R., "An Analytical and Experimental Investigation of Surface Discharges of Heated Water," Hydrodynamics Laboratory, Report No. 135, Boston, Massachusetts, MIT, February, 1971.

15. Koh, R. C. Y., "Two Dimensional Surface Warm Jets," ASCE Journal, Hydraulics Division, 97: HY6, pages 819-834, June, 1971.

16. Schlichting, H., Boundary Layer Theory, Sixth Edition, New York, McGraw-Hill, 1968.

17. Kays, W. M., Convective Heat and Mass Transfer, New York, McGraw-Hill, 1966.

18. Zeller, R., "Summary of Current Theories and Studies Relating to Temperature Prediction," pages 111-156, (see reference 4).

19. Ahlert, R. C. and Nochumson, D., "Oxygen Dynamics in the Thermal Mixing Zone," preprint, presented at the 5th International Water Pollution Research Conference, England, 1970.

20. Chapman, A. J., Heat Transfer, Second Edition, New York, McMillan, 1967.

21. Chu, C. K., "Computational Fluid Dynamics," AIAA Selected Reprints, Series Volume IV, 135 New York, American Institute of Aeronautics and Astronautics, July, 1968.

22. Kurzrock, J. W., "Exact Numerical Solutions of the Time Dependent Compressible Navier-Stokes Equations," CAL Report No. AG-2026-W-1, Buffalo, New York, Cornell Aeronautical Laboratory, February, 1966.